Abstract

This project is focused on the study of concentration of desalination brines, specifically those generated on the desalination of brackish waters using reverse osmosis. When concentrating brines two different objectives are pursued. The first one is to concentrate the brine up to reach the maximum salts concentration, close to saturation, to facilitate the subsequent recovery by a crystallization step. This option is recognized as Zero Liquid Discharge as all the water is evaporated and the solids dissolved are recovered. The second possible objective is the so-called near-ZLD (near Zero Liquid Discharge), consisting in reducing considerably the volume of brine achieving a partial evaporation of the water. The second one is the objective aimed in this project.

As concentration step Membrane Distillation (abbreviated hereafter as MD), an emerging technology integrating membrane and thermal technology will be evaluated. Specifically, the technology to be used is Direct Contact Membrane Distillation (abbreviated as DCMD), in which a hot feed concentrated solution is put in contact with one side of a hydrophobic membrane, on the other side a cold pure water stream is circulated.

The main two advantages of MD are the possibility to operate at low temperatures (e.g. 40 to 60^{o}C) and the capability of working with high concentrations in the feed solution. From the possible problems facing MD three of them have been studied: scaling, temperature polarization and concentration polarization. Scaling consists in the deposition of solid salts on the membrane layer; blocking it and thus decreasing the flow of permeate. In order to avoid the early precipitation of salts different pre-treatments of the brine have been studied and experimented with. To study polarization effects, experiments of distillation modifying operational parameters have been carried out.

The experimental set-up consisted in a membrane module connected in the hot-side to a heated bath, where the feed solution is submerged, and on the cold- side to a refrigerated bath where the distilled solution is cooled down. The mass of distilled water and the temperature in the inlets and outlets of the module have been continuously measured.

To study the influence of the brine pre-treatments an aeration column was built. Brine was treated with different combinations of aeration and acidification. Concentration of the feed solution along the distillation experiments has been analyzed to identify the optimum brine pretreatment.

Experimental data collected in the different experiments have been evaluated according existing theoretical models, being able to evaluate the DCMD method effectiveness to concentrate RO brine, determinate the concentration factors achievable for each pre-treatment, study polarization effects and estimate membrane transport parameters, as well as efficiency indicators.

Contents

1. Nomenclature

T	temperature [^{o}C]
P	pressure [mm Hg]
ΔP	pressure difference [mm Hg]
B	pore tortuosity
J	permeate flux [g/min]
C	membrane permeability [Kg/s·Pa·m^2]
c	concentration [M]
x	molar fraction
K	mass transfer coefficient [m/s]
$E.E.$	evaporation efficiency
Q	heat [W]
H_v	vaporization enthalpy [J/g]
W_{pu}	pumping power [W]
c_p	specific heat [J/g·^{o}C]
k	thermal conductivity [W/m·K]
S	membrane surface [m^2]
d	membrane thickness [m]
v	flow speed [m/s]
m	flow rate [Kg/s]
d_h	hydraulic diameter [m]
$[CO_2]$	concentration of dissolved CO_2 [M]
$[H_2CO_3]$	concentration of carbonic acid [M]
$[HCO_3^-]$	concentration of hydrogen carbonate [M]
$[CO_3^{2-}]$	concentration of carbonate [M]
$[H^+]$	concentration of protons [M]
Re	Reynolds number
Pr	Prandtl number
Nu	Nusselt number
h	heat transfer coefficient [W/m^2·K]
L	length of the membrane [m]
V_A	volume of acid added [mL]

Subscripts

mp	near the membrane (permeate side)
mf	near the membrane (feed side)
p	permeate
f	feed solution
fi	feed solution inlet
fo	feed solution outlet
bf	bulk of feed
bp	bulk of permeate
v	feed solution vapor
o	pure water vapor
l	liquid (here water)
vap	vaporization
T	total
$cond$	conduction
$loss$	heat losses
pu	pumps
max	maximum
h	hydraulic
A	acid
CO_2	carbon dioxide

Greek letters

τ	temperature polarization
ρ	density [Kg/m^3]
μ	viscosity [Kg/m·s]
Θ	contact angle [^{o}]
γ	surface tension [mN/m]

ETSEIB

2. Introduction

Membrane Distillation was invented and patented in 1963 by Bruce R. Brodeli and four years later the first paper was published, in 1967 (Findley, 1967). But it was not until the early 1980s that MD received true interest, with the growth of membrane engineering, when membrane with better characteristics appeared in the market. Since then, an increasing year after year number of papers have been published (Khayet, 2011).

This project is piece inside the cooperative research project between the SETRI-UPC research group and Water Technology Center (CETaqua) devoted to the evaluation of Membrane Distillation as valorization technology of reverse osmosis desalination brines. A preliminary study on the pre-screening evaluation of membrane distillation modules, brine pre-treatments including CO_2 stripping by aeration, acidification to reduce pH to avoid precipitation on the membrane during distillation and using a hollow fiber module liquid contactor was completed recently (Mas, 2014).

This project should be considered a continuation of the previous research project, where a more systematic study on the membrane module performance including temperature and concentration polarization and the use of channel spacers has been carried out. The experimental set-ups and the methodology as well as the data interpretation have been improved including and effort on the process modeling.

It has to be highlighted that there is an increasing interest in this technology for brines treatments and especially on the use of DCMD, the configuration used in this work. In fact, it is the most studied configuration (more than 60% of the studies), and more than 44% of the MD publications are concerned with theoretical models of MD and experimental studies on the effects of the operating conditions (Khayet, 2011) as it has been the objective of this project.

2.1. Objectives

Once the MD module is assembled, the main objective is to recollect data of the working parameters and variables with different types of feed solution. Then these data have to be processed and analyzed with theoretical models describing the different processes involved in direct contact membrane distillation set-ups. As a function of this analysis a set of conclusions will be drawn to describe the behavior of each brine evaluated.

From the data treatment step the membrane transport parameters will be estimated, and with the help of a set of mathematical algorithms the simulation of the polarization of temperature and concentration will be studied. Energy efficiency will also be studied and compared to other existing technologies of brines evaporation.

Finally, collected data of brines pre-treatment will be used to calculate the brines concentration factors. These values will be used to identify the optimum brine pre-treatment.

Summing up, the objectives which are aimed to be achieved are the following:

- Evaluation and calculation of the concentration and temperature polarization.
- Estimation of membrane transport parameters.
- Evaluation of energy efficiency.
- Evaluation of DCMD method on brine concentration.
- Determination of concentration factors for each pre-treatment.

2.2. Scope of the project

The project will be at a laboratory scale, it is not intended to extrapolate the results to industry or to larger facilities. Economics are not going to be studied; environmental impact has neither been studied. Results are expected to give hints on proper choice of working parameters for a higher brine concentration and on pre-treatments. Whether the conclusions can be extrapolated or not to a full industrial scale is not considered part of the project. It is not in the scope of the project to use a heat waste or the use of renewable energy source and heat will be provided using standard water laboratory baths.

3. Concentration of residual brines

One of the biggest problems which society has to cope with nowadays is the distribution of potable water. Less than 3% of the earth's water is fresh and is not distributed in an even way across the planet. Many times the demand of potable water is way higher than the existing resources, and in the poorest areas people do not have access to clean drinking water (Greenlee, 2009). To deal with the challenge of satisficing this increasing demand of water many suppliers are turning toward Reverse Osmosis for desalination of seawater (among other desalination techniques) (Subramani and Jacangelo, 2014).

3.1. Reverse Osmosis

The application of membrane distillation studied in this project is precisely the concentration of rejection concentrate coming from a desalination plant located in Sant Joan Despí. This brine is a waste product of the treatment of surface water from the Llobregat River by reverse osmosis. Llobregat River is characterized at the upper part of the Llobregat basin by a total salinity of 1-2 g/L. A waste flow of brine, with a higher concentration of salts (e.g. 10-20 g/l if the water recovery is 90%) than the inlet of surface seawater is generated.

Osmosis is a physical phenomenon that consists in the movement of water molecules from a less concentrated solution to a higher solute concentration. So if two solutions are put in contact through a semi-porous membrane that only lets water pass through, water will start flowing from the less concentrated solution to the more concentrated one until equilibrium is achieved.

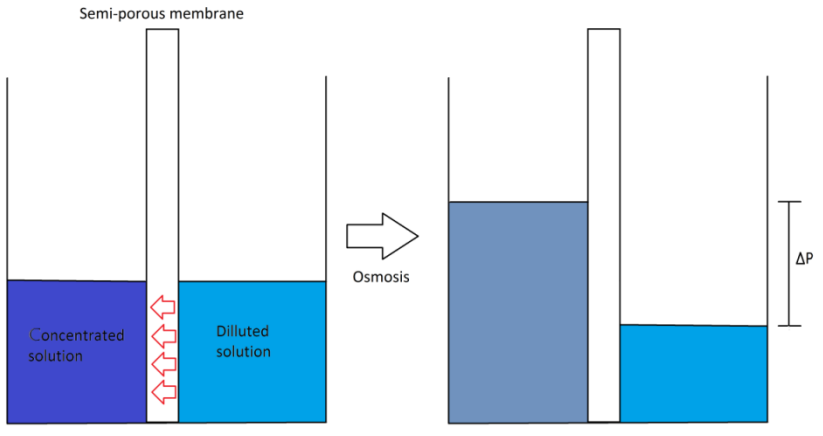

Figure 3-1 Scheme of the osmosis process

Like seen in Figure 3-1 in the equilibrium the forces resulting from pressure differential are equal to the forces resulting from solute and water activity in the membrane.

RO works in the inverse way, pressure is applied on the concentrated side so that water molecules move to the less concentrated side, resulting in desalination of the concentrated water which is concentrated even more. But this has a limit in which is no longer profitable to apply pressure due to flow decay because of concentration. This concentrated brine becomes a waste product that has to be treated and discharged onto the environment avoiding any impact. Brine composition differs a lot depending on the composition of the feed solution and the efficiency of the process. Common disposal options are water discharge, deep well injection, evaporation ponds and land application (Subramani and Jacangelo, 2014). But sometimes these options are no possible (for the case of in-land plants or economically not viable) and here is where different technologies are applied to treat this concentrate.

3.2. Treatment of RO concentrate

There are many different procedures and technologies that are used to treat the RO concentrate, which can be classified as membrane-based, thermal-based, or as emerging technologies. All of them are capable of reducing the volume of concentrate.

<table>
<tr><th>Thermal technologies</th><th colspan="2">Membrane technologies</th><th>Emerging technologies</th></tr>
<tr><td rowspan="2">Multi effect distillation (MED), mechanical vapour compression (MVC) and thermal vapour compression (TVC)</td><td rowspan="2">Pressure-driven membranes</td><td rowspan="2">Electrical potential-driven membranes</td><td rowspan="2">Forward osmosis (FO)</td></tr>
<tr></tr>
<tr><td rowspan="2">Brine concentrator/brine crystallizer</td><td rowspan="2">Intermediate chemical softening</td><td rowspan="3">Electrodialysis (ED) and Electrodialysis reversal (EDR)</td><td rowspan="2">Membrane distillation (MD)</td></tr>
<tr></tr>
<tr><td rowspan="2">Wind Aided Intensified Evaporation (WAIV)</td><td rowspan="2">High efficiency RO</td><td rowspan="2">Thermo-ionic processes</td></tr>
<tr></tr>
<tr><td rowspan="3">Spray dryers</td><td>Intermediate biological reduction</td><td rowspan="3">Electrodialysis metathesis (EDM)</td><td rowspan="3">Eutectic freeze crystallization</td></tr>
<tr><td>Pellet reactors</td></tr>
<tr></tr>
</table>

Table 3-1 Classification of concentration technologies

In Table 3-1 a classification of the different possible technologies and methods can be seen.

Membrane-based technologies require less energy than thermal-based technologies, but when the composition of the concentrate is complex (e.g. in industrial effluents), using membrane-based technologies can be inefficient. Thermal-based technologies consume a larger amount of energy but they are not suitable for large flow rates. Emerging technologies such as forward osmosis and membrane distillation seem to be a good option to treat the concentrate of RO, but still are under development and it is not possible yet to be sure whether on an industrial scale they are profitable or not. Achieving Zero Liquid Discharge has been accomplished with membrane-based and thermal-based technologies or a combination of both.

Any technological solution requires identifying pre-treatment requirements. For instance, treating RO concentrate through membrane or thermal technologies requires removing the scale forming ions and organics, to prevent scaling, fouling and foaming, concepts that will be explained later (Subramani and Jacangelo, 2014).

The basic criterion to select a membrane-based or a thermal-based technology is the total dissolved salt content (TDS). Pressure-driven membranes (like RO) need pressures greater than 82 bars to overcome the osmotic pressure of high TDS (>40g/L). Then, for solutions with high TDS content thermal-based processes and electrical potential-driven membranes are the key to achieve volume minimization or zero liquid discharge, usually thermal-based technologies are combined with a membrane-based stage, but their energy consumption and capital costs are high resulting in substantial treatment costs.

As seen, to achieve ZLD or near-ZLD (95-98% water recovery) one single treatment is not enough (without even taking in account the pre-treatment) and a combination of treatments is necessary, the selection of which is complex and depends on the extent of the concentration process, whether ZLD or near-ZLD, and the characteristics of the RO.

In this project, the technology used to concentrate the brine from RO is one of the above emerging technologies: Membrane Distillation. Applying MD to this waste product it is possible to produce a stream of pure water and a more concentrate stream, which could be crystallized to recover the salts. So, coming from a waste stream it is possible to obtain two valuable products, on one hand pure water, and on the other crystallized salts.

4. Membrane Distillation

Membrane distillation is a thermal separation technique based on membrane technology. Concretely, a porous hydrophobic membrane in direct contact with the flow of liquid to treat is used so that it cannot penetrate through. While the flow of liquid (mostly aqueous solutions) that can be transported through the membrane is zero, the vapor molecules can be transported through the air-filled pores of the membrane, condensing once they reach the other side of the membrane (El-Bourawi et al., 2006).

In order to condensate and to have a driving force, the solution to distillate is set at a higher temperature than the cold side of the membrane, this way the gradient of vapor pressure impulses the flow of vapor, and thus, condensation is possible.

While the flow to treat is always in direct contact there are four main configurations that can be used in the cold side in order to achieve this transmembrane gradient of vapor pressure, as it can be appreciated in Figure 4-1 :

- Direct Contact Membrane Distillation (DCMD): An aqueous solution at a lower temperature than the feed is maintained also in direct contact with the membrane, condensation takes part in this cold flow. The transmembrane temperature difference causes the transmembrane vapor pressure gradient.
- Air Gap Membrane Distillation (AGMD): A stagnant air gap is interposed between the membrane and a condensation surface. This condensation surface is, at the same time, in direct contact with coolant, maintaining a low temperature. In this configuration condensation takes part not in a cold flow but in a cold surface, then permeate is collected.
- Sweeping Gas Membrane Distillation (SGMD): In this configuration, a cold inert gas sweeps the molecules of vapor on the permeate side and then this mixture of gas and vapor is separated in a condenser. The condensation takes part outside the membrane module.
- Vacuum Membrane Distillation (VMD): A pump creates a lower pressure in the permeate side of the membrane. The vacuum applied has to create a lower pressure than the saturation pressure in the feed solution. In this case condensation takes part outside of the membrane module.

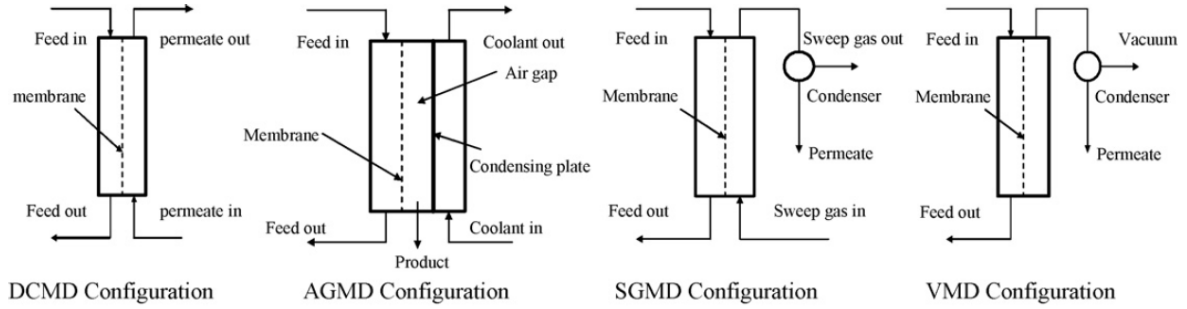

Figure 4-1 Different configurations of MD (El-Bourawi et al., 2006)

Each configuration has its advantages and weak points, but they all have some features in common which distinguish MD: low operating temperatures and low operating pressures.

DCMD is the most studied configuration, as it is the easiest to experiment with due to the fact that condensation occurs inside the membrane module, and that is the reason why this project only studies this configuration despite permeate flux being one of the lowest compared to the other configurations, only superior to AGMD. Otherwise, VMD and SGMD are the least studied, because even if their permeate fluxes are the highest they require external condensers, complicating the system. AGMD configuration, on the other hand, has the lowest permeate flux but heat loss is considerably reduced.

The main benefit of using MD instead of other water treatment technologies is that it can utilize low-grade waste energy sources, like residual water flows at a relatively low temperature (under their boiling point) or alternative energy sources such as solar or geothermal energy.

MD was first patented in 1963 and four years later, in 1967, the first MD paper was published. But at that moment, there was not much interest in this technique as its low permeate rate could not compete with the reverse osmosis technique. In the early 1980s there was a rebirth of interest in MD as membrane production improved a lot and membranes with better features were possible (Andersson, 1985). This alongside with the main benefit of using MD (its low operating temperatures) resulted in a promising objective for research. And since then the amount of papers published on the subject has been increasing year after year (El-Bourawi et al., 2006).

Still, after all the improvements and discoveries, MD has not yet been implemented in industry due to certain problems, such as the low permeate flux compared to other separation techniques like RO, permeate flux decay due to concentration and temperature polarization effects, membrane fouling and pore wetting uncertainty, energetic inefficiency and problematic module and membrane design.

There are three major inefficiencies in MD:

- Temperature and concentration polarization effects.

- Air/gas trapped within the membrane pores, resulting in an additional resistance to mass transfer.
- Heat loss by conduction through the membrane.

As stated before, the thermal energy consumption can be overcame whether by using low energy-sources or waste heat, or also by efficient heat recovery.

MD has been applied (on a laboratory scale) mainly for water reuse and desalination, environmental waste clean-up and in the food industry (juice concentration and milk processing). Desalination is the most popular DCMD application as almost 100% rejection of non-volatile ionic solutes is easily achieved. As seen, all these applications have water as the main component of the feed solution. In Figure 4-2 the different applications suitable for each configuration can be seen.

Summary of the areas where MD process were successfully applied on laboratory scale

Application area	MD configuration			
	DCMD	AGMD	SGMD	VMD
Desalination and pure water production from brackish water	√	√	√	√
Nuclear industry (concentration of radioactive solutions and wastewater treatments; pure water production)	√			
Textile industry (removal of dyes and wastewater treatment)	√			√
Chemical industry (concentration of acids, removal of VOCs from water, separation of azeotropic aqueous mixtures such as alcohol/water mixtures and crystallization)	√	√	√	√
Pharmaceutical and biomedical industries (removal of water from blood and protein solutions, wastewater treatment)	√			
Food industry (concentration of juices and milk processing) and in areas where high temperature applications lead to degradation of process fluids	√	√		√

Figure 4-2 Applications suitable for each configuration (El-Bourawi et al., 2006)

The main advantage of MD over pressure-driven processes such as RO is its ability to treat aqueous feed solutions of very high non-volatile solute concentration, being even capable of recovering valuable crystal products. So MD can be used to recover valuable salts in crystal form from its effluents, then being called MDC (Membrane Distillation Crystallization). MDC differentiates from MD by the presence of a crystallizer, where part of the salts in the supersaturated brine precipitate in crystal form.

4.1. Membrane characteristics

In MD, the membrane acts only as a barrier to hold the liquid/vapor interface at the entrance of the pores and, whereas in other membrane processes the membrane is required to be selective, it is not. Though, the membrane is required to be hydrophobic in order to keep the liquid phase from wetting the pores.

It can be comprised of a single layer or multi-layers, but at least one of the layers should be made of a hydrophobic material and be porous (Khayet, 2011). It is important that the membrane has the lowest resistance to mass transfer possible and the lowest thermal conductivity. Pore size of the membranes used lies between 10 nm and 1µm (El-Bourawi et al., 2006).

Tortuosity factor (measure of the deviation of the pore structure from straight cylindrical pores normal to the surface) should be smaller as possible, as it is inversely proportional to the MD membrane permeability, a value of 2 is frequently assumed (Khayet, 2011).

Porosity should be as high as possible, as it is proportional to membrane permeability. Thickness, however, needs to be optimized as it is inversely proportional to the rate of mass and heat transport through the membrane. Pore size distribution has been rarely studied in DCMD configuration, but it was observed that when using commercial membranes assuming that pore size was constant did not differ much from the results using pore size distribution (El-Bourawi et al., 2006).

The membrane surface contacting the feed solution needs to be resistant to fouling, even though in MD fouling is not as strong as it is in other pressure-driven membrane processes. This resistance to fouling can be achieved by coating the surface with a layer of a fouling resistant material. Membrane should be stable at temperatures as high as 100°C, and have excellent chemical resistance to feed solution and cleaning agents and acids.

Another crucial characteristic of the membrane is the wetting pressure, also known as Liquid Entry Pressure (LEP), which is the limit of pressure that can be applied. If the difference of pressure between the two faces of the membrane is higher than LEP pore wetting may occur. LEP is dependent on the maximum pore size and the membrane hydrophobicity. LEP can be estimated from Equation 4-1 (Franken et al., 1987).

$$\Delta P = P_f - P_p = \frac{-2B\gamma_l \cos\theta}{r_{max}}$$

Equation 4-1 LEP equation

P_f and P_p stand for the hydraulic pressure on the feed and the permeate side, B is the pore tortuosity factor (equal to 1 for cylindrical pores), γ_l is the liquid surface tension, θ stands for the contact angle and r_{max} is the maximum pore size (Alkhudhiri et al., 2012).

So, the membrane has to be hydrophobic and porous at the same time. Polypropylene (PP), Polyethylene (PE), Polytetrafluoroethylene (PTFE) and Polyvinylidene fluoride (PVDF) meet these specifications. Dual-layer hydrophobic-hydrophobic and dual layer hydrophobic-hydrophilic have been also used as well as hollow fibers. Carbon nanotubes have also been introduced within the MD polymer matrix, resulting in a higher porosity and a lower thermal conductivity (Subramani and Jacangelo, 2014).

Still, a stable system distilling correctly can change its behavior just with the presence of surface active components in the feed solution, resulting in the wetting of the pore and permeate purity getting worse. Another trigger for pore wettability would be the transmembrane hydrostatic pressure exceeding the liquid entry pressure (LEP), characteristic of each membrane (El-Bourawi et al., 2006).

The membrane used in experimentation is made of Polyvinylidene fluoride (PVDF), a highly non-reactive thermoplastic produced by the polymerization of vinylidene fluoride with the characteristics that Table 4-1 shows.

Thickness	Contact angle	Geometry	Pore size	Thermal conductivity	LEP	Porosity	Decomposition temperature
110 µm	127^{o}	Single layer (Flat sheet)	0.2 µm	0.19 W/(m*K)	817 kPa	75 %	170 ^{o}C

Table 4-1 Characteristics of the membrane

As seen in Table 4-1, the LEP of the membrane was not known and has been calculated with the Equation 4-1. The LEP has a very high value, which means that just with the applied pressure from the pumps pore wetting will not occur, however, scaling may promote it.

4.2. Temperature and concentration polarization

Temperature polarization is a phenomenon consisting in the difference of temperature between the bulk of the flow and the membrane surface, and concentration polarization consists in a difference between the concentration in the bulk of the feed solution and the concentration of the water in direct contact with the membrane. These differences can be explained by the mass transfer and heat transfer processes that occur inside the DCMD module and have a crucial role on the performance of MD.

4.2.1. Temperature polarization

Temperature polarization is the responsible of most of the loss of MD driving force: vapor pressure. The boundary layer created in each side of the membrane acts as a resistance to heat transfer, and so there is a gradient of temperature between the bulk of the flow and the membrane surface. In fact, up to 80% of reduction in driving force can be observed due to temperature polarization effect (El-Bourawi et al., 2006).

In the simplest model, four thermal resistances can be considered. There are two resistances in the solution due to convection and two more inside the membrane, the resistance due to conduction and the parallel resistance of the vaporization of water on the hot side. The more porous and thermally

insulating the membrane, the higher the proportion of heat resistance in it and thus the higher the difference of temperature in the surfaces. In Figure 4-3 (Alkhudhiri et al., 2012) the different heat resistances can be appreciated.

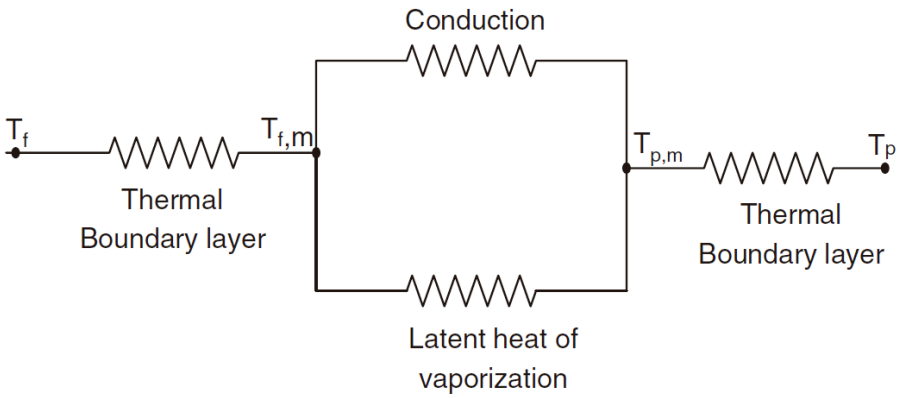

Figure 4-3 Scheme of heat resistances (Alkhudhiri et al., 2012)

Temperature polarization is not a matter of total resistance but of relative resistance, of course, if the total heat resistance is higher, there will be less heat loss.

Temperature polarization coefficient can be defined as the fraction of the transmembrane temperature to the bulk temperature difference (see Equation 4-2) and it gives an idea of the heat efficiency of the module.

$$\tau = \frac{T_{mf} - T_{mp}}{T_{bf} - T_{bp}}$$

Equation 4-2 Temperature polarization coefficient (El-Bourawi et al., 2006)

The curve of temperature that describes the flow can be seen in Figure 4-4. As depicted, there is a substantial change of temperature due to the resistance in convection, to reduce this resistance, the best option is to obtain a flow with less laminar effects, and this can be achieved with the introduction of turbulence promoters like mesh spacers or with higher flows, which result in higher Reynolds number.

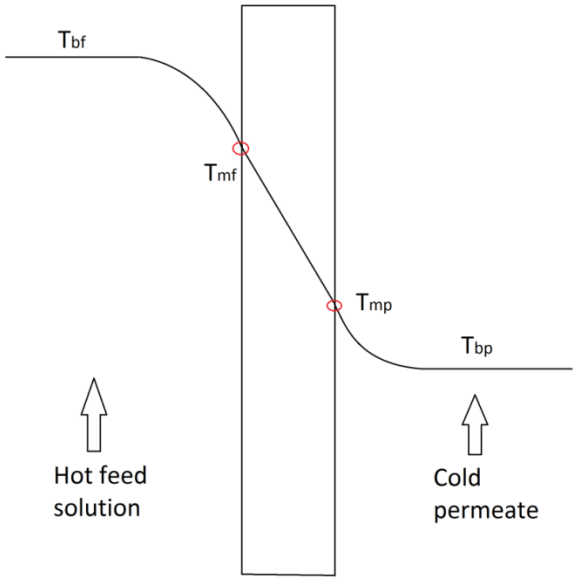

Figure 4-4 Temperature polarization curve

The temperatures in the membrane can be approximated with a basic simulation with MATLAB. With the temperatures in the membrane it is possible to calculate the vapor pressure and so the driving force. The Equation 4-3 explains the relation between the flux and the difference of vapor pressure.

$$J = C \cdot (P_{mf} - P_{mp})$$

Equation 4-3 Flow and differential of pressure

Where J is the permeate flux, P_{mf} and P_{mp} are the vapor pressures in each side of the membrane and C is the membrane permeability, which is approximately constant (Chan et al., 2005).

4.2.2. Concentration polarization

Another form of polarization is the one that affects the concentration, this polarization is characteristic for a higher concentration of the species dissolved in the feed solution when closer to the boundary layer, which acts as an additional resistance to mass transfer.

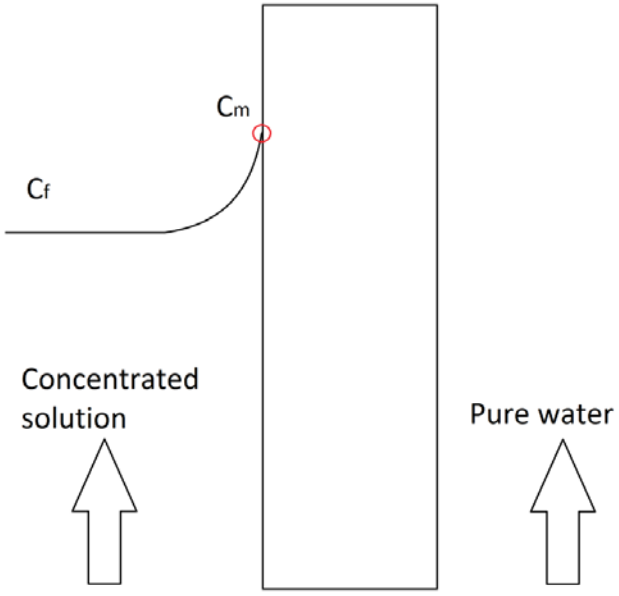

Figure 4-5 Concentration polarization

In Figure 4-5, the higher concentration of the feed solution when closer to the membrane can be appreciated. This polarization also affects the difference of vapor pressures because when a solution is more concentrated its vapor pressure is diminished. In Equation 4-4 this phenomenon can be observed for NaCl solutions.

$$P = P_0 \cdot (1 - x) \cdot (1 - 0{,}5 \cdot x - 10 \cdot x^2)$$

Equation 4-4 Vapor pressure for NaCl solutions (Martinetti et al., 2009)

So, as the solution in contact with the membrane has a lower vapor pressure, the differential of vapor pressures from side to side of the membrane has decreased respect to the differential that there would be if the vapor pressure was the same as in the bulk of the flow. Equation 4-5 gives the concentration of the dissolved species in the membrane surface.

$$c_{mf} = c_{bf} \cdot e^{(\frac{J}{\rho_f K})}$$

Equation 4-5 Concentration polarization (Alkhudhiri et al., 2012)

Where c_{mf} is the concentration in the membrane surface, c_{bf} stands for the concentration on the bulk of the feed solution, J is the flow of permeate, ρ_f is the density of the liquid and K is the mass transfer coefficient.

4.3. Scaling and fouling

Fouling is defined as the formation of deposit on the membrane surface. It is one of the major obstacles of MD, with the consequence of flux decay throughout time.

Fouling results in a decrease of the membrane permeability and heat resistance due to the deposition of suspended or dissolved substances on the membrane surface and/or inside the pores. Different types of fouling include:

- Organic and biological fouling.
- Particulate and colloidal fouling.
- Inorganic fouling, also known as scaling.

Organic fouling consists in the deposition of dissolved material, whereas particulate fouling is the deposition of solids in suspension on the membrane. Scaling occurs when the ionic product of sparingly soluble salts in the concentrated exceed the equilibrium solubility product, an example of scaling of $CaCO_3$ is depicted in Figure 4-6.
Scaling will be the type of fouling predominant in experimentation, as the concentration of ions in brine is much higher than the concentration of organic species and particles and its effects will be much greater. When distilling, the supersaturation state allows the nucleation and crystal growth (Pokrovsky, 1998), and if the solute solubility increases with temperature there will be deposition due to temperature polarization and concentration polarization, as seen in Figure 4-6. For salts with inverse solubility characteristics maximum super saturation occurs in the bulk of the flow rather than at the membrane surface. This can cause plugging of the membrane pores entrances causing first flux decay and may lead to membrane pore wetting, which consists in the entrance of the feed solution inside the pore (Gryta, 2008).

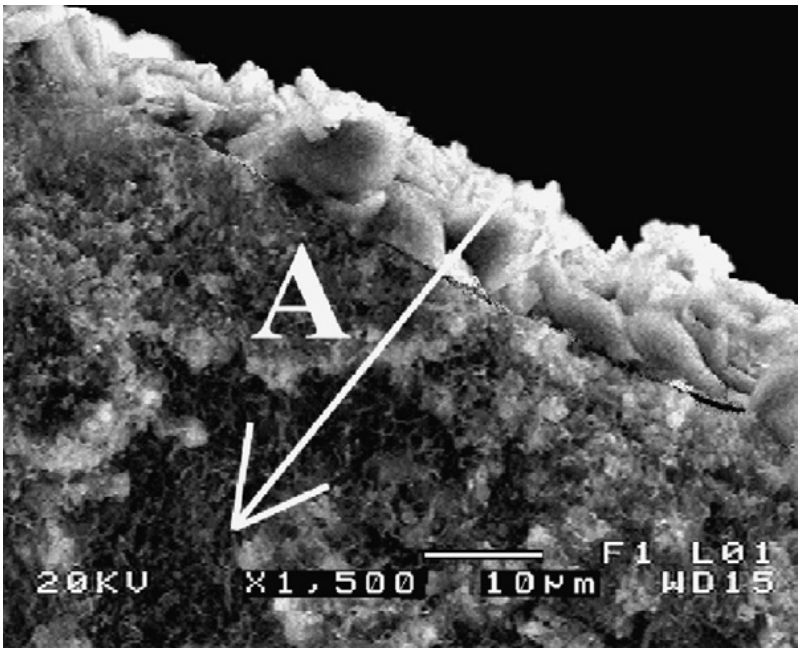

Figure 4-6 Scaling of $CaCO_3$ on a membrane (Gryta, 2008)

Furthermore, this deposition of ionic salts can eventually result in an increase in the pressure drop to levels that the hydrostatic trans-membrane pressure may exceed the LEP and promote pore wetting (El-Bourawi et al., 2006).

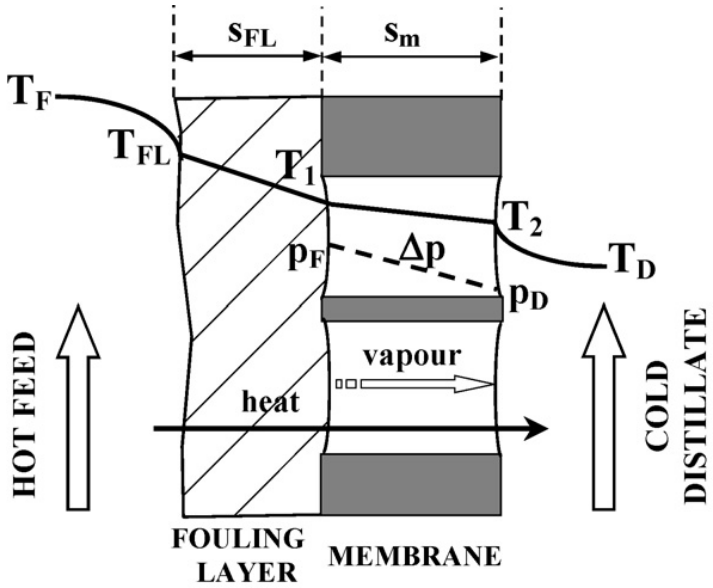

Figure 4-7 Scaling on the membrane (Gryta, 2008)

In MD, in order to work conveniently, a thin layer of air entrapped in the membrane pores is necessary for a smooth running operation. A scaling layer formed on the membrane surface causes progressive wettability of the membrane, thus decreasing its porosity and permeability, and so, the permeate flux. It also has a less important effect of increasing heat resistance, see Figure 4-7. This phenomenon is accelerated if salt crystals are formed inside the pores. As stated before, organic fouling is not as important as scaling. In fact, fouling caused by humic acids (one of the main components of organic matter in water and wastewater) was less serious in MD processes than in other membrane processes (Gryta, 2008).

There are two methods to avoid scaling and other types of fouling: periodic cleaning of the membrane and pre-treatment of the brine, section 5 is focused on pre-treatment of the brine, periodic cleaning was not considered as an option in the experimental setting, the amount of experiments would have been too high.

4.4. Energetic efficiency

MD's main advantage over other distilling and desalination techniques is its low operating temperatures. But even if these temperatures are so low, the feed and permeate are very close in space, in fact, in DCMD they are only separated by a thin layer of the order of 100 µm. This closeness is the responsible of the major heat inefficiency of DCMD: losses by conduction (Bui et al., 2007).
In order to quantify the losses by conduction in the module, evaporation efficiency is usually introduced in the energetic evaluation, see Equation 4-6.

$$E.E. = \frac{Q_{vap}}{Q_T} = \frac{Q_{vap}}{Q_{vap} + Q_{cond}}$$

Equation 4-6 Evaporation efficiency (Bui et al., 2007)

Evaporation efficiency is the fraction of energy transmitted in the module that is actually used for the distilling of the feed solution. Part of the heat transmitted is wasted in conduction through the membrane. Another fraction of the heat transmitted is lost through the module surface and heat leaks, and finally part of the energy is used for evaporating the volume of feed solution that then condenses and becomes permeate. But evaporation efficiency only takes into account the heat of conduction and the heat of vaporization.

In Equation 4-6, Q_{vap} stands for the heat of vaporization, Q_{cond} stands for the heat of conduction and Q_T is the total heat exchanged in the module (without heat losses). Q_{vap}, Q_{cond} and Q_T can be calculated from the set of equations Equation 4-7, Equation 4-8 and Equation 4-9, where H_{vap} stands for the vaporization enthalpy, C_p is the specific heat, T_f and T_p the mean temperatures of feed and permeate, k the thermal conductivity, S the surface of the membrane, d the thickness of the membrane, T_{fm} and T_{pm} the temperatures on the membrane of the feed and permeate side, m the mass flux (of both

permeate and feed solutions), T_{fi} and T_{fo} the temperatures of the inlet and the outlet of the feed solution and T_{po} and T_{pi} the temperatures of the inlet and the outlet of the permeate solution.

$$Q_{vap} = J \cdot (H_{vap} + c_P \cdot (T_{bf} - T_{bp}))$$

Equation 4-7 Vaporization heat

$$Q_{cond} = \frac{k \cdot (T_{mf} - T_{mp}) \cdot S}{d}$$

Equation 4-8 Conduction heat

$$Q_T = C_P \cdot \dot{m} \cdot (T_{fi} - T_{fo}) - Q_{loss} = C_P \cdot \dot{m} \cdot (T_{po} - T_{pi}) = Q_{cond} + Q_{vap}$$

Equation 4-9 Total heat

Another indicator of energetic efficiency is energy consumption per flow rate of permeate. As its name suggests, it gives an idea of how much energy it takes to distillate a unit of mass of permeate, or how much power does it take to distillate at a certain flow rate. Depending on the criterion of the authors the energy spent can be the thermal energy to heat the feed solution and cool down the permeate (Criscuoli et al., 2008) or the mechanical energy to pump the solutions if the energy to heat and cool down is obtained from waste or solar sources, see Equation 4-10, where W_{pu} stands for the mechanical energy of the pumps and J stands for the flux of permeate.
Depending on the criterion chosen, the differences between the results can be notable, as more than 90% of the energy consumption is related to heating and cooling (Chiam and Sarbatly, 2013).

$$Energy\ consumption = \frac{\dot{W_{pu}}}{J}$$

Equation 4-10 Energy consumption per unit of permeate

5. Pretreatment of the brine

As explained in section 4, one of the major problems of membrane distillation is flux decay. In this project this flux decay is given by the accumulation of precipitated salts on the membrane surface. Scaling can be avoided or at least delayed by the modification of working parameters, but also by applying a suitable pretreatment.

But before choosing a pre-treatment first it has to be taken into account which kind of brine it is and what is its composition. An analysis of the main components of the RO brine is collected in Table 5-1.

Cations	Anions
925 ppm Na^+	1890 ppm Cl^-
665 ppm Ca^{2+}	1470 ppm SO_4^{2-}
213 ppm Mg^{2+}	1230 ppm HCO_3^-
193 ppm K^+	97 ppm NO_3^-

Table 5-1 Chemical composition of the RO brine

As the river quality changes daily due to climatological conditions the composition of the RO brines changes and along the project each sample used for the experiments was analyzed to determine the concentration of the main components. Additionally, brine contained from 10 to 15 mg/L of a polyphosphonate antiscalant. Its concentration was estimated, as there are not robust analytical techniques to determine its concentration in brines.

So, taking a glance at the concentrations, it is clear that the presence of hydrogen carbonate can promote scaling with Ca(II) and Mg(II) ions precipitating calcium and magnesium carbonates even with the presence of antiscalant (which is utilized at the RO process to avoid scaling) (Pokrovsky, 1998). So one of the first species to precipitate will probably be carbonate salts.

5.1. Carbonic system

Carbonic acid is a weak diprotic acid (pK_{a2} 10.3 and pK_{a1} 6.3). Overall, the equilibrium of the system can be summed up by Equation 5-1, Equation 5-2, Equation 5-3, Equation 5-4 and Equation 5-5.

$$CO_{2(g)} \leftrightarrow CO_{2(aq)}$$

$$CO_{2(aq)} + H_2O_{(l)} \leftrightarrow H_2CO_{3(aq)}$$

$$H_2CO_{3(aq)} \leftrightarrow HCO^-_{3(aq)} + H^+_{(aq)}$$

$$HCO_{3(aq)}^{-} \leftrightarrow CO_{3(aq)}^{2-} + H_{(aq)}^{+}$$

Equation 5-1 Carbonic system

$$\frac{P_{CO_2}}{[CO_2]} = 29.41 \frac{L \cdot atm}{mol}$$

Equation 5-2 Absorption equilibrium (Henry's law)

$$\frac{[H_2CO_3]}{[CO_2]} = 7 \cdot 10^{-7}$$

Equation 5-3 Acid carbonic equilibrium

$$\frac{[HCO_3^-] \cdot [H^+]}{[H_2CO_3]} = 10^{-6.3} \frac{mol}{L}$$

Equation 5-4 First proton dissociation

$$\frac{[CO_3^{2-}] \cdot [H^+]}{[HCO_3^-]} = 10^{-10.3} \frac{mol}{L}$$

Equation 5-5 Second proton dissociation

As seen in the reactions in Equation 5-1, pH has a vital role and its effect can be appreciated in Figure 5-1.

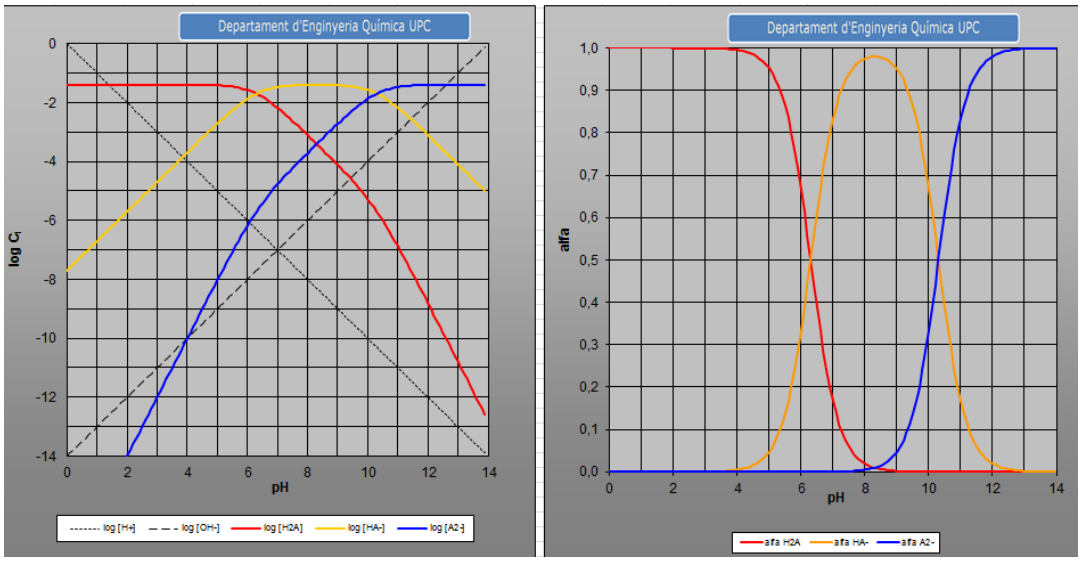

Figure 5-1 Logarithmic diagram of concentrations and diagram of alpha composition

In Figure 5-1 the total concentration of carbon species was 0.04 M, which is the result found in the RO brine used in the experiments during the concentration assays.

In the membrane module, the concentration rises up to a point in which precipitation of calcium and magnesium carbonate is not avoidable. To try to avoid this, two methods of pre-treatments have been studied: acidification and aeration.

5.2. Brine acidification with hydrochloric acid

Acidification consists in addition of a strong acid to the feed solution (e.g. HCl or H_2SO_4). Usually the first acid is the one used as the second increases probabilities of scaling of sulfate species (Karakulski and Gryta, 2005).

If the pH of the solution is decreased more carbon will be in hydrogen carbonate and carbonic acid. This carbonic acid will easily decompose in water and CO_2 will leave the solution depending on the partial pressure of the gas phase in contact with the solution. With the common atmosphere and its low partial pressure of carbon dioxide most of it will leave the solution.

So the concentration of carbonate will be lower both because the total inorganic carbon concentration will be lower and because less percentage of it will be in form of carbonate. This difficults precipitation as the product of concentrations is lower, but the problem of this method is that it requires a high consumption of acid in order to decrease pH from 7-8 (the initial pH) to pH=4, point in which practically all inorganic carbon has left the solution or is in form of dissolved CO_2, see Figure 5-1.

With acidification it is possible to avoid the precipitation of $CaCO_3$, but even if the concentration of CO_3^{2-} is reduced, the concentration of Ca^{2+} remains the same. This means that if calcium is in a solution with a high concentration of SO_4^{2-} it could still precipitate, in the form of $CaSO_4$ (Qu et al., 2009).

5.3. Brine aeration

Another possibility is to aerate the solution using compressed air. This way the desorption process of CO_2 dissolved in the solution is accelerated and the CO_2 is absorbed by air since it has a lower partial pressure than the pressure needed to reach equilibrium with the solution (Lisitsin et al., 2008).

This stripping of CO_2 has two different effects. On one hand the total concentration of inorganic carbon diminishes. On the other hand, the pH rises, up to the point in which the concentration of bicarbonate is enough to start precipitation of $CaCO_3$ and/or $MgCO_3$.

The maximum pH that can be achieved by air stripping is restricted by the CO_2 content of ambient air. This restriction is given by the equilibrium of the partial pressure of CO_2 gas and its corresponding concentration in the solution. This equilibrium follows Henry's law, see Equation 5-2 (Cohen and

Kirchmann, 2004). If another pure gas was used the total stripping of the CO_2 would be possible and the pH would rise up to a maximum value that would depend on the initial concentration of inorganic carbon.

These pretreatments can be combined with acidification in various ways to improve their effectiveness. There are a few different combinations:

- Acidification and later aeration: acidification promotes almost all inorganic carbon to be in dissolved CO_2 and then aeration strips it.
- Long aeration with filtration and later acidification: Aeration is applied to the solution until the equilibrium is reached (with precipitation included). Then this solution is filtrated and acidified. Inorganic carbon will leave the solution both by CO_2 stripping and by precipitation. Calcium and/or Magnesium are reduced by precipitation. Next, acidification reduces the high pH created by aeration.
- Acidification, aeration and then acidification again: if the pH is reduced again then it will be more difficult to precipitate throughout MD.
- Aeration at a constant pH: With this method the rate of CO2 stripped will be higher, but the volume of acid spent will be higher too.
- Short aeration without precipitation and later acidification: The volume of acid spent is minor but the Calcium and/or Magnesium is not eliminated.

6. Experimental methodology and procedures

The experimentation carried out can be separated in two stages, in the first stage solutions without any kind of pre-treatment to the feed solution were used, whereas in the second stage brines had been pre-treated. For both stages the MD experimental methodologies and procedure was the same.

6.1. Study of the most effective parameters in MD

In the first stage, without brine pre-treating, there have been evaluated the two main parameters affecting the permeate flux: feed solution flow-rate and the presence or not of channel spacers. Attempts were made in order to maintain constant the temperatures of the feed solution and the cold side, but small fluctuations appear from experiment to experiment. The reason to maintain the temperature constant is to limit the number of experiments to be carried out in the time scope of the present project. Furthermore, temperature has been extensively studied in the literature, while with the use of spacers and the flow rate it will be possible to study temperature polarization effects.

So, a total of four experiments were carried out with three different feed solutions. The first series of experiments was made with distilled water, the second with a solution of Sodium Chloride (200 g /L water) and the third with un-treated brine from the Drinking Water Plant of Sant Joan Despí.

The two first series have been carried out with distilled water and NaCl solution so concentration polarization effects can be observed and whether it is negligible or not as it is suggested (Chan et al., 2005). The last series of experiments have been carried out with brine to decide the conditions of flow rate and the use of channel spacers for the second stage of experimentation.

6.2. Study of the pretreated brine

In this second stage of experimentation with MD, the feed solution has been pretreated with either acidification or aeration, or a combination of both. The aim of these experiments has been to determine up to which point can be concentrated the brines and which is the method that allows a higher concentration of the brine without precipitating. The procedure has been the same as in the first stage of experimentation but including the monitoring of composition of the treated brine along the concentration step.

6.3. Physical assembly of the MD module

The most important point of the physical assembly of the MD set-up is the choice of the method of measuring the permeate flux. It was decided that it would be measured as the mass (registered every few seconds with a balance with data logger) that overflowed from a Büchner flask that had been pierced and attached to a tube, see Figure 6-1. In this way the distilled water accumulated in the Büchner falls to a beaker, placed over a balance (Mettler Toledo PG503-S Delta Range) that registers, by using a PC computer, the mass increase with time.

Figure 6-1 Büchner flask modified to improve overflowing

The hot circuit was chosen to be in the downside, in order to try to facilitate ascension through the membrane of trapped gases and vapors.

Feed solution is placed in a glass container submerged in a heated bath of water, the temperature of which can be regulated appropriately. The distilled water stream that is used in the cold side is placed in the Büchner flask, as described before. All the connections have been done with plastic tubes, metallic clamps and plastic bridles. The tubes for the pumps are made of silicone, because they have to bear with constant deformations from the movement of the two peristaltic pumps (07553-75 Masterflex).

Four thermometers have been incorporated; one for each inlet and outlet, so temperature can be monitored with time. Due to this, it was observed that just with the heated bath (J.P. Selecta Digiterm 100) and the refrigerator (J.P. Selecta 3001214) used in the cold side temperatures were not the

desired ones. Temperatures of 60°C and 20°C were expected, but they barely reached 40°C and 30°C. To solve this limitation a new design of a refrigeration coil made from copper pipes for the permeate side and another coil (made of glass) was attached to the hot side. In this way the temperature could be increased up to 54°C in the hot side and the temperature desired of 20°C in the cold side was achieved. The cold side works with a refrigerator with a probe in direct contact with the solution, whereas in the heated side the controller regulates the temperature of the water in the bath, not in the solution.

These temperatures were considered valid on account of the following reasons:

- The cold temperature, 20°C, is the cold temperature par excellence. Is the nearest to ambient temperature, and the most used at most consulted references.
- The hot temperature, 60°C, is more difficult to justify. At the beginning a temperature of 60°C in the inlet of the module was desired, but then, as explained before, a higher temperature would be needed at the heated bath, causing massive losses by evaporation, with the ulterior refills of water, colder than the bath, resulting in fluctuations in the temperature. If a lower temperature had been used, the experiments would have taken more time, and polarization effects would have been less obvious. Furthermore, 50°C-60°C is a representation of the temperature of a residual flow with energy.

Figure 6-2 Configuration on the cold side on the left and freezing of the refrigerator on the right

In Figure 6-2 an initial configuration of the cold side can be observed, but as shown, the higher the volume the more difficult it was for the refrigerator to handle with the heat coming from the module,

and even with stirring (J.P. Selecta 5050111 RZR-1), it would freeze. From this point on, stirring was added to the cold side.

Figure 6-3 Another failed configuration

Figure 6-4 Refrigerating coil

In Figure 6-3 there is one example of the first attempts, there are no thermometers, neither any coils, and so the surface of heat transfer was not enough to maintain the desired temperatures. It can also be observed that the MD module is in a higher position, resulting in longer tubes. In this attempt, the volume of the refrigeration bath had been reduced and there was stirring (not seen in the picture though) so that the refrigerator would not freeze. In Figure 6-4 the details of the refrigeration coil can

be seen, the solution enters the coil at approximately 26 ^{o}C, depending on the experimental conditions (flow rate and channel spacers), and leaves at 20 ^{o}C.

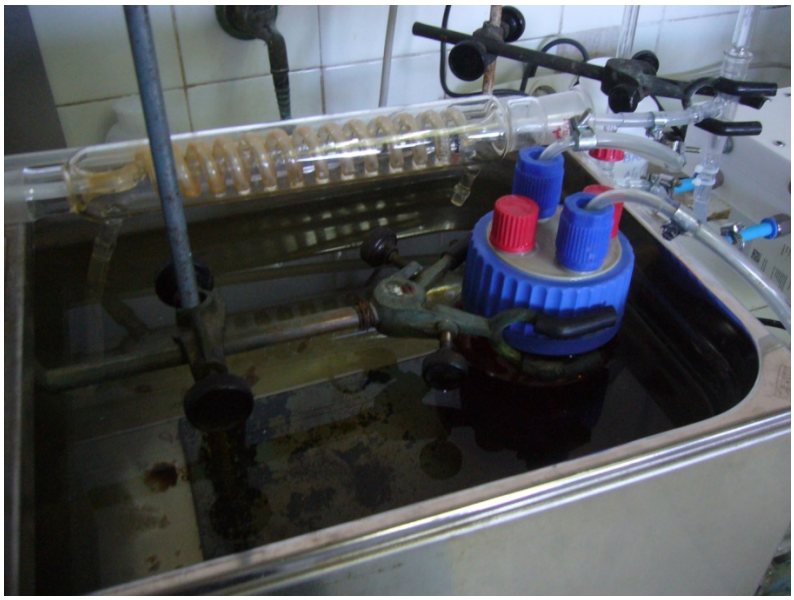

Figure 6-5 Final configuration on the hot side

In Figure 6-5 there is depicted the detail of the heated bath, with the feed solution container submerged in it. It can also be observed the heating glass coil and, in the top right of the picture, the inlet and outlet of the module with their respective thermometers. This is the final configuration. It must be pointed out that this is how it looked in the beginning, after some experiments the distilled water of the bath oxidized the iron stand that holds the container and the water turned red. This oxidization could have made a layer of oxide in the heating coil, resulting in a less heat exchange efficiency, but that was not considered as a major problem.

So, in the final configuration, see Figure 6-6, there are four thermometers and a box under the module to level it. The final configuration of the cold side with the Büchner can be seen in Figure 6-7, with the refrigerating copper coil, the probe of the refrigerator inside the Büchner and the balance.

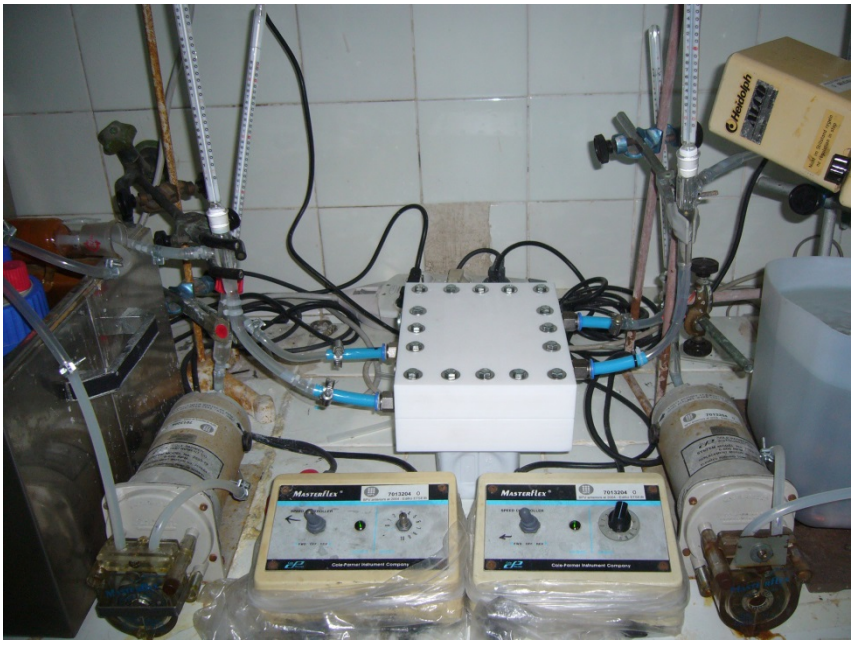

Figure 6-6 Final configuration of the module

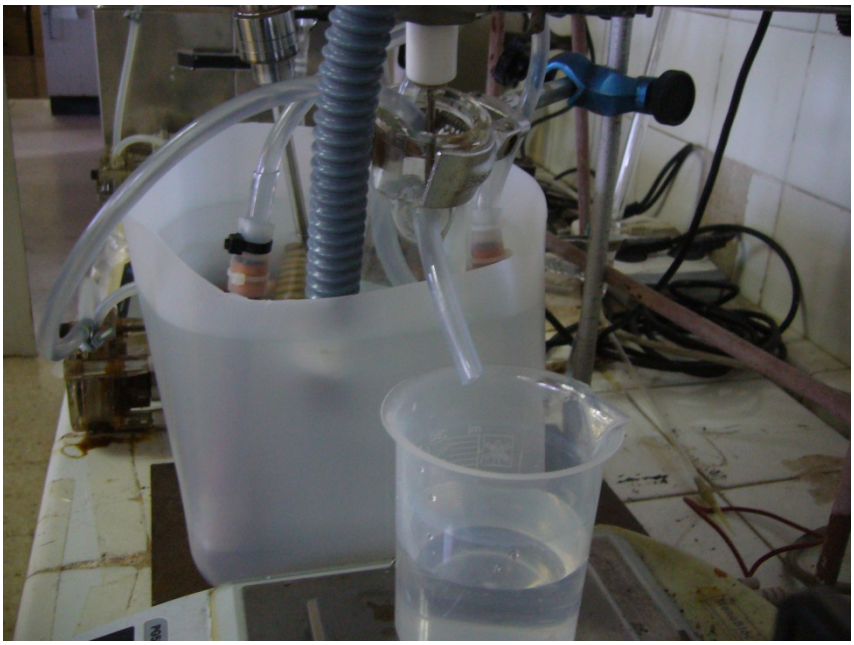

Figure 6-7 Final configuration of the cold side

6.4. Experimental methodology in the MD studies

First thing to be done was to turn on the heating bath and the refrigerator of the cooling bath, as well as the stirring of the later. The computer was turned on and the balance connected to it. Then, the

membrane was appropriately cut from the coil of PVDF (10413096 from Westran S) and placed inside the module and channel spacers were placed too when necessary. Finally, the screws were screwed with a screwdriver until they were tight and not liquid leakage was observed. Then the module was connected with the inlets and outlets pipes.
The conductivity of the feed solution was measured with the Conductimeter GLP 31 and the pH with the pH Meter GLP 22 from Crison.
When the heated bath had achieved the desired temperature, 63.5^{o}C, depending on the volume of the batch two different procedures were followed:

A) If the volume was 500 mL, this volume of the feed solution was loaded into the feed solution container being measured with a graduated cylinder with a total capacity of 1 L. The container was covered with a cap and submerged inside the heated bath up to the neck of the container. It was left to heat half an hour and then pumping of the feed solution and permeate was slowly started.

B) If the volume was 930 mL, the maximum of feed solution possible was loaded into the container. The container was then covered and submerged and let to heat. When pumping had started and all the volume of air inside the pipes and the module had left the container was refilled up to the maximum, achieving the total volume of 930 mL.

It has to be noted that both pumps had to work in the same direction, otherwise the flows would be counter-current and it is known from the former project in MD that this membrane tends to tear apart with counter-current flows.

With a smaller graduated volumetric flask of 100 mL and a chronometer the flows were measured by measuring the time that it took to pump 100 mL in the case of high flow rate or 50 mL in the case of low flow rate. If the calculated flow rate was not the desired, the controllers were regulated and the flow rate was measured again, and this was repeated until the desired flow rate was the one achieved. This was done both for the pump of the cold circuit and the hot circuit.

Once the flow rates had been established, the temperatures in the inlets and outlets were left to stabilize, the Büchner flask was screeded, a beaker was placed in the balance, the tare was done and the data logger turned on.
This was considered the beginning of the experiment, from this point every 30 minutes or 1 hour, depending on the length of the experiment, the temperature data were collected and samples were taken following one of the following procedures:

A) If pH was not considered relevant, 4 mL were simply pipetted from the container unscrewing one of the four small caps it had. Of these 4 mL, 2 mL were necessary for the TOC analysis, and the rest were necessary for the analysis of chromatography. After that the cap was screwed back.

B) If the pH was measured, the pipe of return from the module of the feed solution side was unscrewed and placed in a 50 mL container. Next, the pipe of return was screwed back into the container. In this recipient the pH was measured and 4 mL were pipetted for subsequent analysis, the rest was returned into the container.

Along each experiment and more water being evaporated the beaker filled up to the point where its content could spill out. At that point it had to be emptied and the tare was done again. This procedure is limited by the fact that as maximum 500 g could be weighted with the required accuracy.

When air was present in the pipes (which were transparent) it meant that the volume of feed solution left was not enough to fill all the volume of the circuit, and the experiment was finished at this point. The experiment could also be finished if the membrane was blocked because fouling problems, so if there had not been an increase in the distilled mass for the last half of hour the experiment was finished.

At the end of each experiment the pH and conductivity of the permeate were measured and the two circuits were emptied. Next the module was disassembled and cleaned; the membrane was stored for further analysis of XRD+SEM.

In the feed circuit hydrochloric acid was pumped at an approximated concentration of 0.01M prepared in the laboratory from a mother solution of 1M. Next distilled water was pumped to clean any acid left.

6.5. Matlab algorithm

A Matlab algorithm was programmed to calculate the theoretical temperatures at the membrane surface. For simplicity, the algorithm only works with water as feed solution and its temperature close to 50^{o}C, the temperature of permeate has to be close to 20^{O}C. Otherwise the properties of the fluids would not be the ones assigned in the algorithm. These conditions have been selected as they could be the expected conditions if this system is implemented at industrial scale. However, the algorithm could be modified appropriately if other temperatures on the hot and could circuits were selected.

The function *itertemp* has the inlet arguments *J,FR,Tbf,Tbp,* which stand for permeate flux (introduced in mL/min), flow rate (L/min), mean temperature of the bulk of the feed solution and mean temperature of the bulk of the permeate (both in ^{O}C). Once these have been defined, the first thing that the function does is to assign values to the thermodynamic properties of the fluids and the

parameters of the module. These thermodynamic properties are exclusive for the temperatures chosen and for pure water, and should not be extrapolated to other temperatures or other feed solutions if the same degree of accuracy is pursued.

Then, it calculates the Reynolds and Prandtl of each flow with Equation 6-1 and Equation 6-2 . Next, the Nusselt number of each flow is calculated from the expression in Equation 6-3 (Khayet, 2011), where d_h stands for the hydraulic diameter and L stands for the length of the membrane.

$$Re = \frac{d_h \cdot v \cdot \rho}{\mu_i}$$

Equation 6-1 Reynolds number

$$Pr = \frac{c_p \cdot \mu}{k}$$

Equation 6-2 Prandtl number

$$Nu = 1.86 \cdot \left(\frac{Re \cdot Pr \cdot d_h}{L}\right)^{\frac{1}{3}}$$

Equation 6-3 Nusselt expression (Khayet, 2011)

With the Nusselt numbers, the heat transfer coefficients of each flow can be calculated with Equation 6-4.

$$h = \frac{Nu \cdot k}{d_h}$$

Equation 6-4 Heat transfer coefficient

Then, the heat transfer coefficient of vaporization is calculated with Equation 6-5, the values of the bulk temperatures are assigned to T_{mf} and T_{mp} in order to start the iteration. And once all the heat transfer coefficients have been calculated the first iteration can be done.

$$h_{vap} = \frac{J \cdot H_{vap}}{(T_{mf} - T_{mp})}$$

Equation 6-5 Heat transfer coefficient of vaporization

The new values of temperatures of the membrane surfaces are found with Equation 6-6 and Equation 6-7 (Martínez-Díez and Vázquez-González, 1999).

$$T_{mf} = T_{bf} - (T_{bf} - T_{bp}) \cdot \frac{\frac{1}{h_f}}{\frac{1}{h_p} + \frac{1}{h_f} + \frac{1}{h_{vap} + \frac{k}{d}}}$$

Equation 6-6 Temperature of the membrane on the feed side (Martínez-Díez and Vázquez-González, 1999)

$$T_{mp} = T_{bp} + (T_{bf} - T_{bp}) \cdot \frac{\frac{1}{h_p}}{\frac{1}{h_p} + \frac{1}{h_f} + \frac{1}{h_{vap} + \frac{k}{d}}}$$

Equation 6-7 Temperature of the membrane on the permeate side (Martínez-Díez and Vázquez-González, 1999)

After these new values are calculated, the heat transfer coefficient of vaporization is recalculated with Equation 6-5. Then, temperatures are recalculated with Equation 6-6 and Equation 6-7, and so on until the module of the difference between the two temperatures in one iteration and the following iteration are minor than the *err* value (chosen to be 10^{-20}).

6.6. Design and assembling of the aeration column

A PMMA pipe of 1.5 meters of length and 144 mm of diameter and with a total volume of 24.4 Liters was used. A PMMA cylinder was attached together to it, providing a union between the column and the base, which was mechanized from a thick sheet of PMMA, to which holes were drilled to introduce screws (the union was also drilled) and to provide two ducts communicated with the outside to connect the pipe to obtain samples and the pipe where air flows. Furthermore between the column and the basis a rubber joint was placed to assure tightness. The air pipe in the inside of the column was connected to a diffuser that guaranteed proper uniform distribution of small air bubbles, favoring specific surface and desorption processes. This diffusor was stuck to the bottom of the column with double-faced duct tape. To obtain a better visual idea of the set-up, see Figure 6-8.

Figure 6-8 Aeration column set-up

6.7. Experimental procedure of the aeration

Before starting any experiment the column was disassembled to clean any rest of precipitate from a former experiment. 11 Liters of brine were deposited inside the column so that it was half filled: enough filled to favor the desorption processes but not too much to prevent the brine from overflowing.
The brine volume was measured with a graduation incorporated to the column body. The accuracy of this graduation is in the order of 1 ±0.1 L. Following, air bubbling is carried out with a compressor (Herkules Green Silent from Nuair), attached to the entrance pipe and the flow rate measurer. The aeration was done with a steady flow rate of 2 Nm^3/h during a maximum time of 40 minutes (maximum time of continuous operation of the compressor to avoid heat up problems)

Along the experiments, samples were extracted from the column using a sampling pipe. When sampling a purge was applied to be sure that the solution measured was the one in the column and not the one in the pipe. Approximately 50 mL of sample were taken and immediately measured its pH. Then turbidity analysis was done with 10 mL of this sample to control whether or not there was precipitate in the sample. Finally, 4 mL were stored for TOC and chromatography analysis.

In some experiments, precipitation appeared. So, the volume to be distilled had to be filtrated. In this case 2 L of the aerated solution were filtrated with a Büchner flask, a Kitasato, filter paper and a vacuum pump, and then stored in two flasks of 1 L. Even though only 930 mL were necessary it was decided to store 2 L to have extra volume, to practice more than one posterior treatment and to have a spare volume in case an additional experiment in the MD module was necessary.

The turbidimetry analysis was done with the Turbidity Meter LP 2000 from Hanna Instruments. The pH analysis was done with a pH Meter GLP 22 from Crison, in stationary working mode.

It has to be noted that the study of the aeration process was not in the scope of this project.

6.8. Sample analyses

In both aeration and MD experimentation samples were taken to determine their composition, specially:

- The total inorganic carbon (including dissolved carbon dioxide, carbonic acid, hydrogen carbonate and carbonate).
- The total organic content, account for the organic matter present on the brines

- Major anions and cations: Sodium, Magnesium, Calcium, Chloride and Sulfate.

6.8.1. Total organic and inorganic content (TOC/IC) analyses

Samples taken were diluted with a constant dilution factor of 8.5 for the MD experiments; 15 mL of ultra-pure distilled water were added to 2 mL of sample. This dilution factor was chosen so that all measures were in the range of maximum precision of the TOC analyzer (TOC-VCPH from Shimadzu) and that there was enough volume to make more than one measure.
Every three or four samples a blank was analyzed to detect any malfunction of the analyzer. Furthermore, the calibration was performed with standards solutions with concentrations of 1, 5, 10 and 100 mg C/L, with an accuracy ± 0.1 mgC/L.

The total inorganic content for samples at pH values below the pK_{a1} had associated higher errors, especially if samples are not measured following its sampling as most of the inorganic content is lost from the aqueous sample. The results considered in this work are the ones belonging to the B1, A'2, MM1, MM2 and NN series.

6.8.2. Chromatography analyses

Ion chromatography (Dionex ICS-1000 Thermo Scientific) was used to measure the concentration of Sodium, Magnesium, Calcium, Chloride and Sulfate. Standard solutions used for calibration covered the range from 3 ppm to 300 ppm.

Before the analysis samples were diluted appropriately efforts were made in the calculation of the dilution factor so that the measured value was in the middle of the calibration curve, this way the measure would have the highest accuracy.

Once the dilution factors had been calculated, the samples were diluted and the solution was filtered with a syringe and a filter of 0.2 µm, the solution was introduced in a chromatography vial. In the analysis protocol blank samples were intercalated between samples to detect malfunctioning.

The results considered in this work are the ones belonging to the B1, A'2, B2, MM1, MM2 and NN series.

7. Results and data interpretation

As stated before, the experimentation can be divided in two blocks, one concerning the mass and heat transfer phenomena as well as the characterization of the system parameters and another one dealing with the concentration of the brine and its composition throughout time.

The first block has three series: Distilled water (with code D), Solution of NaCl (with code S) and Brine (with code A), although one of the experiments of these last series is also studied in the second block.

7.1. Mass and heat transfer phenomena evaluation (experiments D, S, A)

In these series the experiments took place without prior treatment to the model brine solutions. In Table 7-1 details on the experimental conditions used are provided.

	Distilled water	NaCl solution	Brine
Low flow rate, no spacers	D1	S1	A1
High flow rate, no spacers	D2	S2	A2 and A2'*
Low flow rate, presence of spacers	D3	S3	A3
High flow rate, presence of spacers	D4	S4 and S4'*	A4

Table 7-1 Classification of experiments

*Some of the experiments were repeated.

The low flow rate experiments were carried out with an approximate flow rate of 0.22 L/min whereas the high flow rate experiments were carried out with an approximate flow rate of 0.55 L/min. These two flow rate are characterized with a Reynolds number of approximately 97 and 240 for water and brine (density of the brine can be considered equal to the water's). However, the introduction of spacers provokes a more turbulent flow.

These flow rates were controlled in the beginning of the experiment and not continuously, and this could be a major cause of deviation in experiments with the same conditions.

7.1.1. Distilled water series (D)

In these series, the feed solution running on the hot side was pure distilled water (500 mL), just like the solution running on the cold side, as a result, in the module there was not concentration polarization neither membrane blocking due to precipitation in the pore entrances. Data of the evolution of the distilled water as a function of time are shown in Figure 7-1.

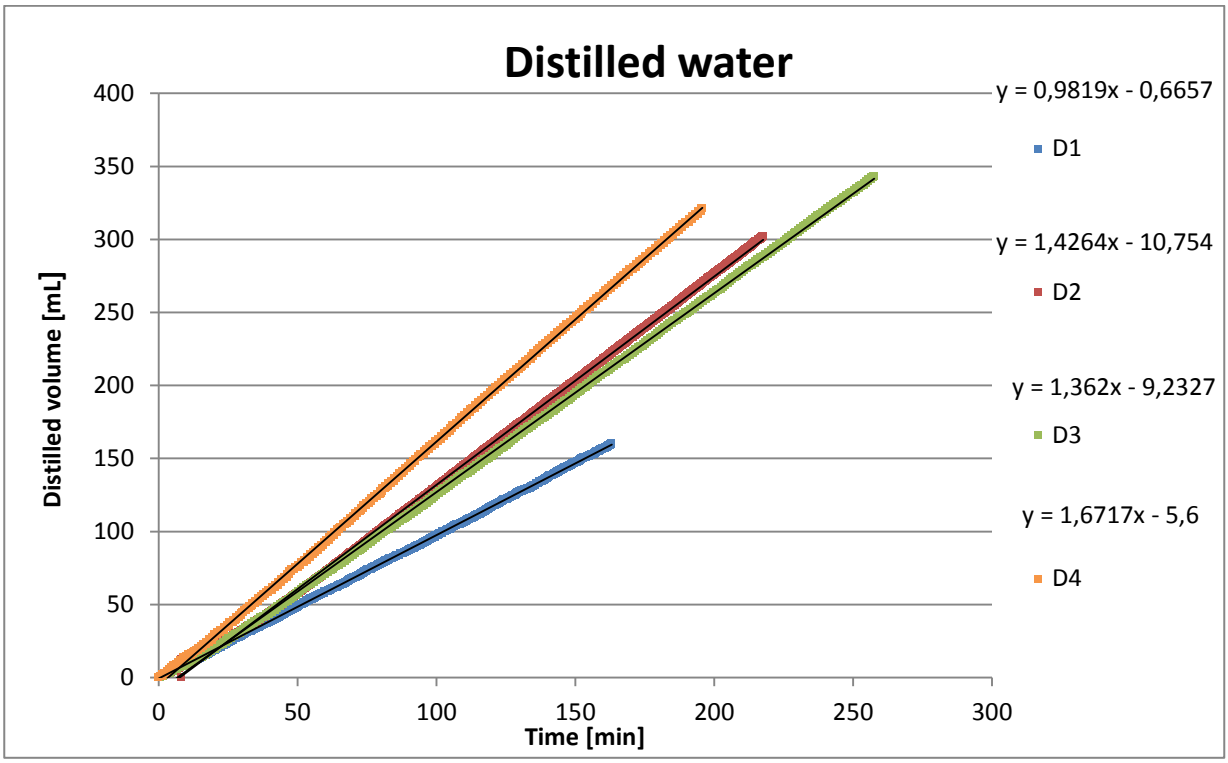

Figure 7-1 Distilled volume vs time

The evolution of the distilled water with time can clearly be approximated as a lineal one (with a R^2 factor greater than 0.999), fact that suggests that for pure water as feed stream the permeate flux remains constant. This is due to two causes: on one hand, there is no concentration polarization, which just as solution volume decreased would become more severe. On the other hand, precipitation over the membrane is avoided and so the subsequent blocking of the pores.

If the apparent straight line is zoomed, three levels of curve can be appreciated:

1. The first level, in which a straight line can be clearly appreciated, is the interesting curve for the study of parameters and results; see Figure 7-1.
2. In the second level, what used to look like a straight curve now has a sinusoidal component, with a period of 25 minutes, just like the refrigeration period of switch-on and shutdown. The refrigeration unit is automatically switched on when the temperature of the probe, which indicates the temperature of the inlet of permeate into the module, rises higher than 20°C, and is automatically shut down when the temperature of the probe is lower than 20°C. These little variations of the inlet temperature of the cold circuit result in little variations of the driving force, generating thus little changes in the permeate flux and thus the sinusoidal curve. See Figure 7-2.

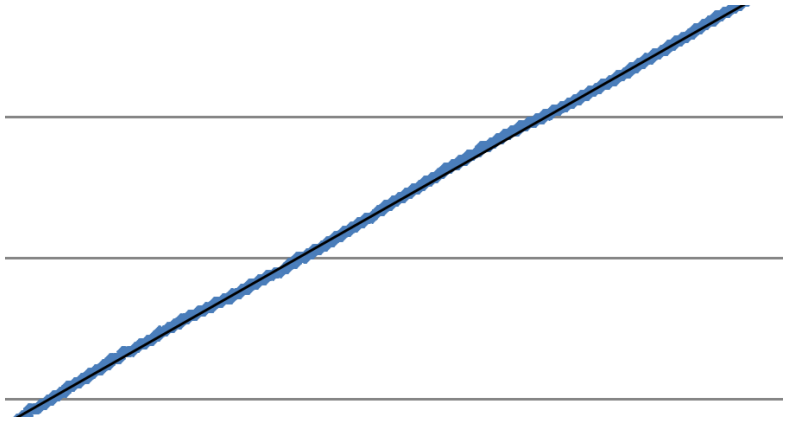

Figure 7-2 Zoomed curve

3. In the third level of zoom, the previous continuous curve is suddenly stepped in discrete levels, see Figure 7-3. This is a consequence of the overflow method, in which the permeate flux is not continuous.

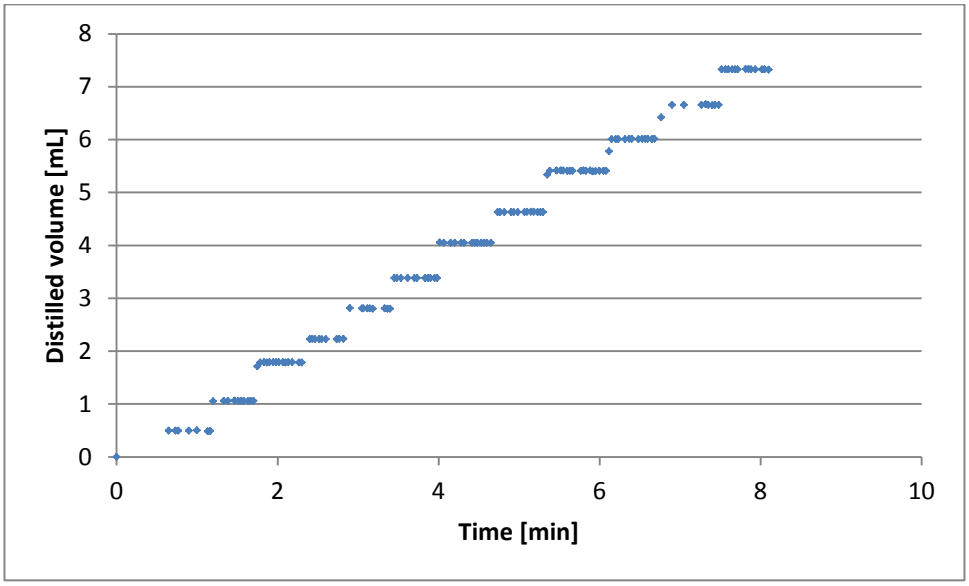

Figure 7-3 More zoomed curve

Regarding the amount of water that has been possible to distillate, it has no real limit. As the feed solution is pure water, there is no obstacle to unstopped distillation and zero liquid discharge could be achieved. The only reason for not being achieved is the fact that there is a minimum amount of volume for the liquid to fill up the circuit, if more volume of the initial 500 mL is distilled, air enters in the module and conditions change to worse, resulting in an undesired configuration.

With the slopes of the regression lines the fluxes of permeate are found, and it is possible to see how increases with the increase of the flow rates and with the introduction of spacers. This could be

explained considering that: when the flow rate is increased and/or spacers are introduced, the flow becomes more turbulent and less laminar, decreasing the laminar effects and the thickness of the boundary layer. And it is in the boundary layer where the temperature polarization effects occur. However, these permeate fluxes cannot be compared directly, because if the flow rate is increased the outlet temperatures change and so the pressure gradients change too. Despite this, it is possible to obtain a preliminary estimation of the tendencies because temperatures do not change much. Table 7-2 shows the evolution of the temperatures for the four series of experiments.

	T_{fi} [°C]	T_{fo} [°C]	T_{bf} [°C]	T_{pi} [°C]	T_{po} [°C]	T_{bp} [°C]
D1	54	45	**49.5**	20	26	**23**
D2	54	49	**51.5**	19	23	**21**
D3	54	45	**49.5**	20	27	**23.5**
D4	53	49	**51**	20	24	**22**

Table 7-2 Temperatures of the inlets and outlets of each experiment

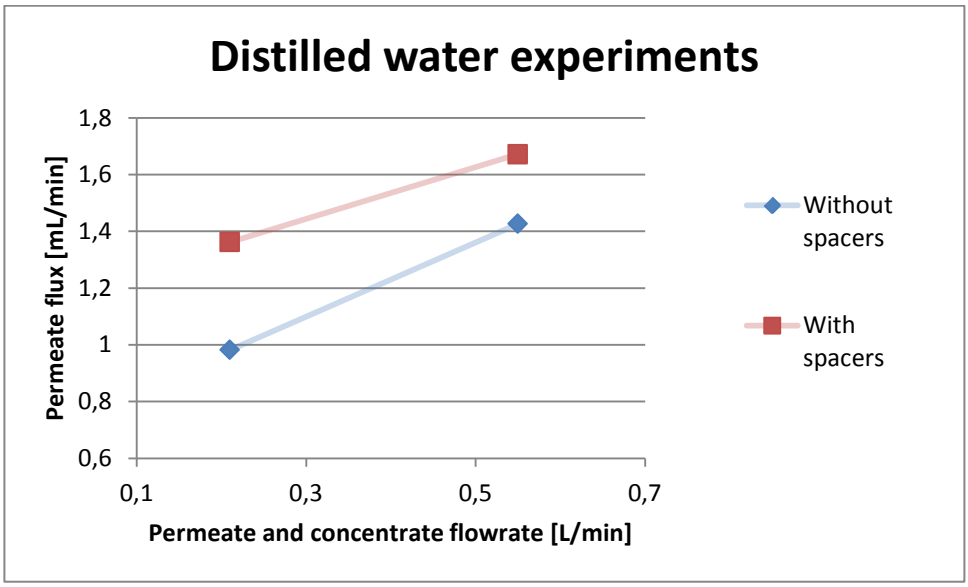

Figure 7-4 Flow rate for each experiment

	D1	D2	D3	D4
D1	0	+45.3%	+38.7%	+70.2%
D2	-	0	-4.5%	+17.1%
D3	-	-	0	+22.7%
D4	-	-	-	0

Table 7-3 Relative increases of permeate flux

In Figure 7-4 there is depicted a representation of the measured distilled flow rate for the experiments at high and low flow rate for Reynolds numbers of 239 and 97 approximately. As

expected, distilled flux increases due to reduction of laminar effects. The presence of spacers results in a higher permeate flux for both low flow rate and high flow rate, but the effect for the low flow rate is more accentuated.

In Table 7-3 there can be seen a comparison of the relative increases of permeate flux for each experiment. Then, results on Figure 7-4 and Table 7-3 confirmed the observed results in Figure 7-1. D4 has the higher permeate flux, a 70% higher than D1 and 23% than D2, when the flow rate is increased with the presence of spacers the increase of permeate flux is minor than without the use of spacers. The increase in D2 respect D1 is the double than that of D4 respect D3 (+45% versus +23%).

The reason for this difference in the improvement is associated to the increase of the needed turbulence to promote the decrease of the temperature polarization. In Figure 7-4 both curves, represented as straight lines because there were only two points, would end up to a maximum value at high Reynolds numbers. So, the higher the Reynolds number of the flow is, the lower the increase of permeate flux will be when spacers are introduced or the flow rate is increased.

Calculus of temperature polarization and membrane permeability

For the calculations of the membrane permeability and the temperature polarization coefficient a mean temperature has been considered as the temperature of the bulk. Therefore the simulation and calculus process could be simplified without supposing a sacrifice on the accuracy of the estimated and calculated parameters. The mean temperature values have been calculated with the temperatures of the inlet and outlet of both the hot and cold system.

To calculate the membrane temperature, as explained previously, the mean temperatures and parameters of the experiment (feed solution, flow rate) were used as input values of the numerical algorithm written in MATLAB. Calculated theoretical temperatures in the surface of the membrane were used to calculate the polarization factor and the vapor pressures.

	T_{fi} [°C]	T_{fo} [°C]	T_{pi} [°C]	T_{po} [°C]	T_{mf} [°C]	T_{mp} [°C]	τ
D1	54	45	20	26	41.6	30.4	**0.42**
D2	54	49	19	23	43.5	28.5	**0.49**
D3	54	45	20	27	-	-	-
D4	53	49	20	24	-	-	-

Table 7-4 Temperatures of the flow and the membrane

In Table 7-4 flow temperatures for each experiment and the polarization temperatures for the experiments in which channel spacers were not used are collected. The calculation of polarization temperature for experiments using channel spacers was not performed due to the complexity of the system. Despite of the fact that D2 and D3 seem to have a similar turbulence (regarding the permeate flux) D3 and D4 have not been considered in the calculus of the permeability coefficient because the boundary layer effects are unknown and a more complex numerical simulation should have been used.

The polarization factor, see Table 7-4, increases in D2 (0.49) respect D1 (0.42), proving that a higher Reynolds number results in a higher heat efficiency.

From the polarization temperatures the vapor pressure can be obtained with the Antoine equation, and so, the membrane permeability coefficient. The permeate flux (J) has been calculated taking into account the area used (12 cm per 7.5 cm).

	Permeate flux [Kg/m^{2}h]	P_{mf} [mm Hg]	P_{mp} [mm Hg]	ΔP [mm Hg]
D1	6.546	60.0	32.5	27.5
D2	9.509	66.3	29.1	37.1

Table 7-5 Permeate flux and pressures, obtained with the Antoine law

In Table 7-5, the driving forces are calculated, and as expected, the driving force of the less laminar flow experiment is higher than that of the more laminar flow experiment. The membrane permeability (C) was calculated using Equation 4-3.

In Table 7-6 the permeability coefficients for each experiment and the mean are collected.

	C [Kg/m^{2}s·Pa]
D1	$5.03 \cdot 10^{-7}$
D2	$5.41 \cdot 10^{-7}$
Mean	**$5.22 \cdot 10^{-7}$**

Table 7-6 Membrane permeability

Comparing the result of $5.22 \cdot 10^{-7}$ Kg/m^{2}s·Pa with values of (Martínez-Díez and Vázquez-González, 1999), who found a permeability of $14.5 \cdot 10^{-7}$ Kg/m^{2}s·Pa for a slightly different membrane of PTFE (80% void fraction, 60 µm of thickness, 0.2 µm nominal pore size). These two values differ due to the different membrane material and characteristics, but have the same order of magnitude.

(Mas, 2014) found a value of $16.7 \cdot 10^{-7}$ Kg/m^{2}s·Pa with exactly the same membrane of PVDF used in this study. These differences may be explained because of the higher control of inlet and outlet temperatures and permeate flux. (Chan et al., 2005) found a value of C equal to $3.8 \cdot 10^{-7}$ Kg/m^{2}s·Pa with a membrane of PVDF (porosity 70%, nominal pore size 0.22 µm and thickness of 125 µm), the membrane was very similar to the one used in this work (porosity of 75%, nominal pore size of 0.22 µm and thickness of 110 µm). The agreement between both values is a confirmation on the algorithm used.

7.1.2. Concentration of NaCl solutions (series S)

In this set of experiments, the same operating conditions were used to concentrate 500 mL of a solution of sodium chloride with the aim of: a) studying the evolution of permeate flux with the presence of salts and b) studying the precipitation of salt into the membrane surface using a high

concentration of salt to determine whether it is possible to identify the point in which precipitation starts.

The feed solution used was a solution of sodium chloride with an approximate concentration of 3.2 M (100g in 500mL of water), which is a concentration close to the saturation (5.9 M, 180 g in 500mL of water at 25^{o}C). The following parameters are expected to change in this set of experiments:

- There is a decrease in the vapor pressure due to the presence of concentrated salts.
- Concentration polarization appears, increasing the concentration of salts in the membrane and thus decreasing more the vapor pressure.
- Precipitation occurs and so scaling.
- Temperature polarization calculus is no longer an option as all thermodynamic and physic-chemical properties change and become dependent on temperature and concentration. Temperature polarization should be calculated then with complex numerical methods simulations, which are not in the scope of this project. There is also expected the scaling phenomena, which modifies the properties of the membrane.
- Temperature polarization calculus becomes also too complex at these high concentrations, because mass transport coefficients have to be recalculated.

Despite all of these limitations, the results on the evolution of the distilled water volume with distillation time are plotted in Figure 7-5, where it can be noticed that the curve is completely different than that of the distilled water.

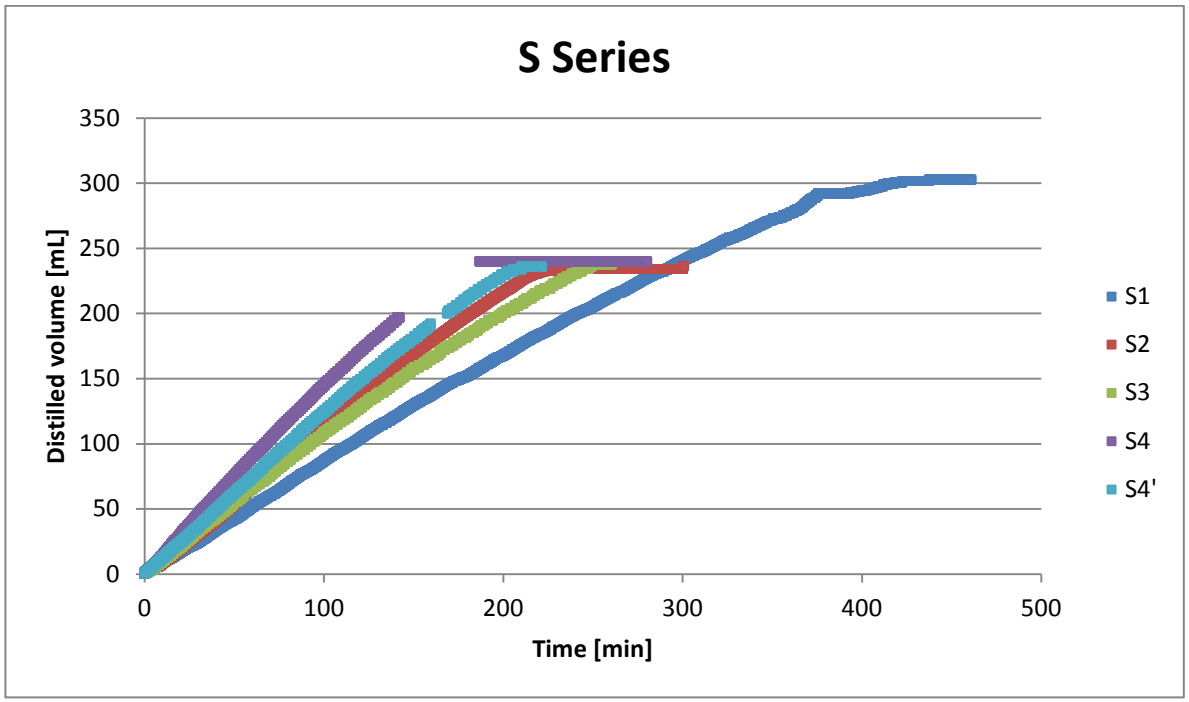

Figure 7-5 S Series: Distilled volume versus Time

Figure 7-5 shows that three of the experiments have a limited value of distilled volume, with its corresponding concentration factor. On the other hand, S1 allows a higher concentration of the feed solution up to higher maximum value of distilled volume. This result is associated to membrane blocking. In Table 7-8 the different concentration factors achieved in each experiment are collected. As seen, the concentration factors of the experiments are almost the same; with the exception of S1, with a higher concentration factor.

	S1	S2	S3	S4	S4’
CF	2.38	1.81	1.84	1.82	1.85

Table 7-7 Concentration factors for each experiment

It is also possible to observe how permeate flux increases or decreases among the experiments. The tendencies are the same than those with distilled water: S4 and S4’ (the repetition of S4) are the ones with a higher permeate flux. The difference between S4 and S4’ is due to the fact that in one of the experiments the flow rate could not be measured at the initial stage of the experiment. These two are followed by S2, which also took place with high flow rate but without spacers. These two are followed by S3 and S1, the same order as in D series. The permeate flux of the S series can be compared directly just like D series because its temperatures are very similar as it is shown in Table 7-8.

	T_{fi} [°C]	T_{fo} [°C]	T_{bf} [°C]	T_{pi} [°C]	T_{po} [°C]	T_{bp} [°C]
S1	54	48	**51**	19	25	**22**
S2	53	51	**52**	19	22	**20.5**
S3	54	47	**50.5**	21	27	**24**
S4	53	49	**51**	20	24	**22**
S4’	51	48	**49.5**	19	23	**21**

Table 7-8 Inlet temperatures, outlet temperatures and mean temperatures

The reason why S1, even having a lower permeate flux allows a higher concentration of the solution are the conditions in which it took place. It seems that a more laminar flow promotes the crystallization in bigger particles than when precipitation occurs in more turbulent flows, where the nuclei are smaller. These smaller nuclei can bloke the pore easier as their dimensions are similar, with the medium pore size being 0.22 µm. However, if the crystals are smaller, they have much more difficulty to block the pore, resulting in retarded total membrane blocking as seen in experiment S1 (Chan et al., 2005).

But even if looking at the time evolution of distilled water volume function (Figure 7-5) it is possible to see when the membrane blocks, it is not possible to determine at which point precipitation starts, which was one of the aims of these experiment series. And so, in order to determine when precipitation occurs in further experiments, chromatography was used instead of detecting by monitoring the evolution of the volume of distilled water.

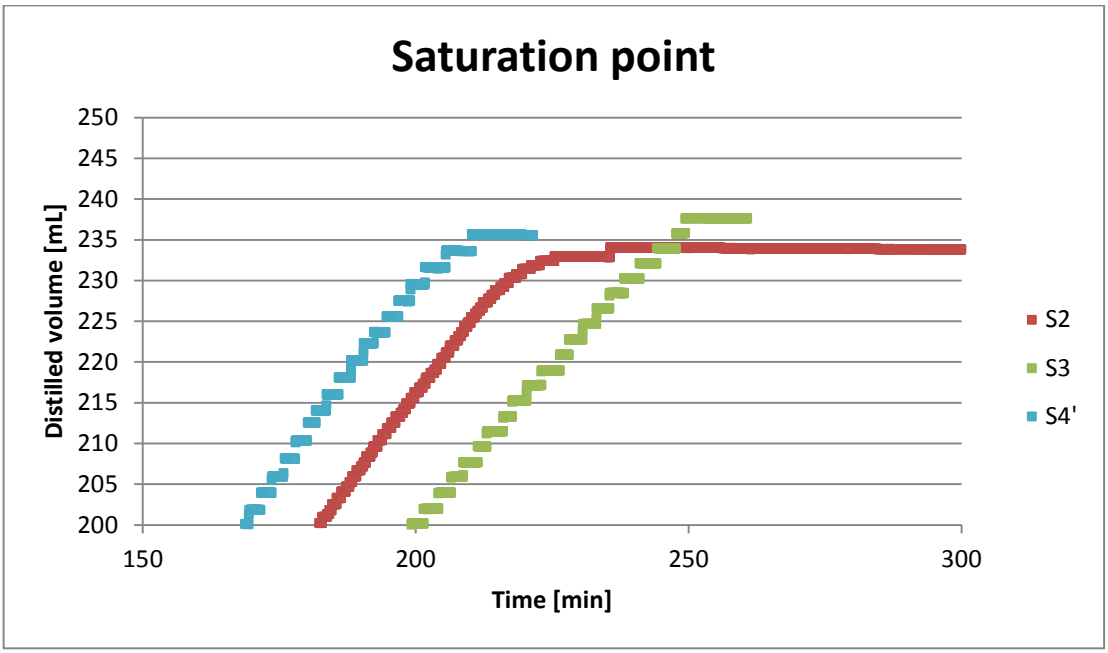

Figure 7-6 Distilled volume curves near the point of saturation (222 mL)

In all experiments, just after the distilled volume reaches the saturation point the permeate flux is reduced drastically, as seen in Figure 7-6. This confirms the hypothesis of flux decay (e.g approaching to zero net flux) due to pore blocking due to the precipitation of sodium chloride. This precipitation is accelerated by concentration polarization, which increases the concentration on the membrane, allowing local saturation at the liquid film in contact with the membrane surface even if the feed bulk solution is not yet at the point of saturation. Crystallization takes place over the membrane and then promoting a progressive pore blocking. The process is not instantaneous, otherwise the volume limitation would be before 222 mL and it is actually further than that, at approximately 235 mL. Precipitation in other points of the circuit can also play a role in the delay of the blocking; salt was found in the feed solution container.

Figure 7-7 Crystallization over the membrane and the module (S1)

In Figure 7-7 there can be seen the membrane and the module after the experiment, with big crystals accumulated on both of them, the difference is obvious when compared to the crystallization over the experiments in S3, in Figure 7-8.

Figure 7-8 Crystallization over the spacer and the membrane (S3)

Comparison between concentration experiments with water and NaCl solutions (D Series and S Series)

Apart from evaluate whether it was possible or not to determine where the precipitation occurred just from the time evolution of distilled water volume function, the experiments with sodium chloride were carried out to quantify how could influence the presence of salts in the efficiency of the distillation.

To isolate the effects of the presence of dissolved salts, the time-lapse in which there was not precipitation, or at least, theoretically there was not, data have been used.

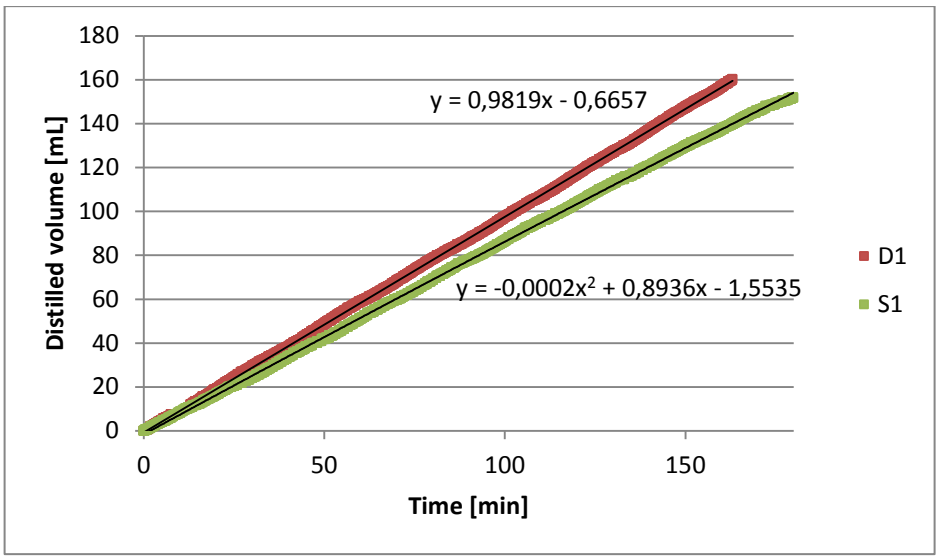

Figure 7-9 Distillate volume in D1 and S1

In Figure 7-9, D1 distilled water fluxes can be considered constant as the function volume of distilled water with time is following a linear relationship; however, at the end S1 has a parabolic behavior and has to be explained by a more complex phenomena. D1 has a higher permeate flux, an average 14% higher than S1.This is due to the fact that the feed solution is very concentrated and it affects the vapor pressure by decreasing it. The parabolic behavior can also be explained by this concentration. The more concentrated the feed solution, the lower its vapor pressure and so the permeate flux. Concentration polarization also has a decreasing effect here, as it gets more and more accentuated through the experiment and makes the concentration in the membrane to be higher, decreasing even more the vapor pressure. But the main responsible for the reduction of flux is the vapor pressure suppression due to the high concentration of the salt, concentration polarization plays a marginal role (Ali et al., 2013).

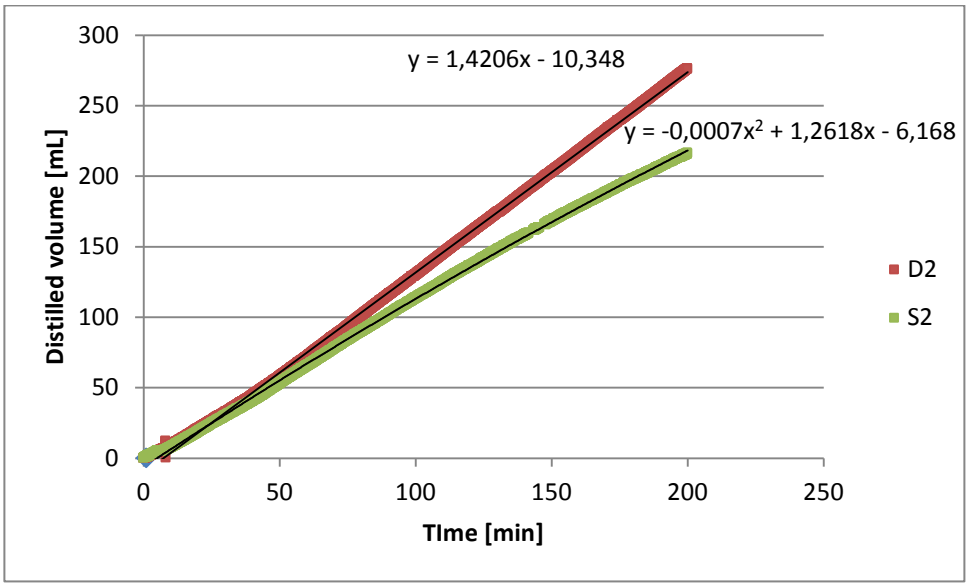

Figure 7-10 Distillate volume in D2 and S2

In Figure 7-10, Figure 7-11 and Figure 7-12 the same distillation curves are observed with the same flux decreasing behavior, where with the increase of time the reduction of the flux is seen due to both the influence of the salt concentration and concentration polarization.

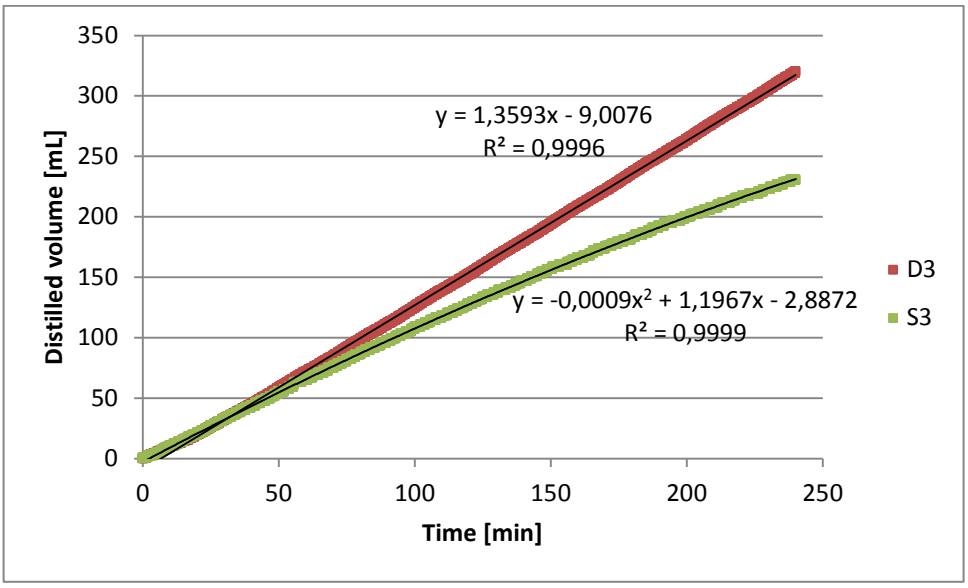

Figure 7-11 Distillate volume in D3 and S3

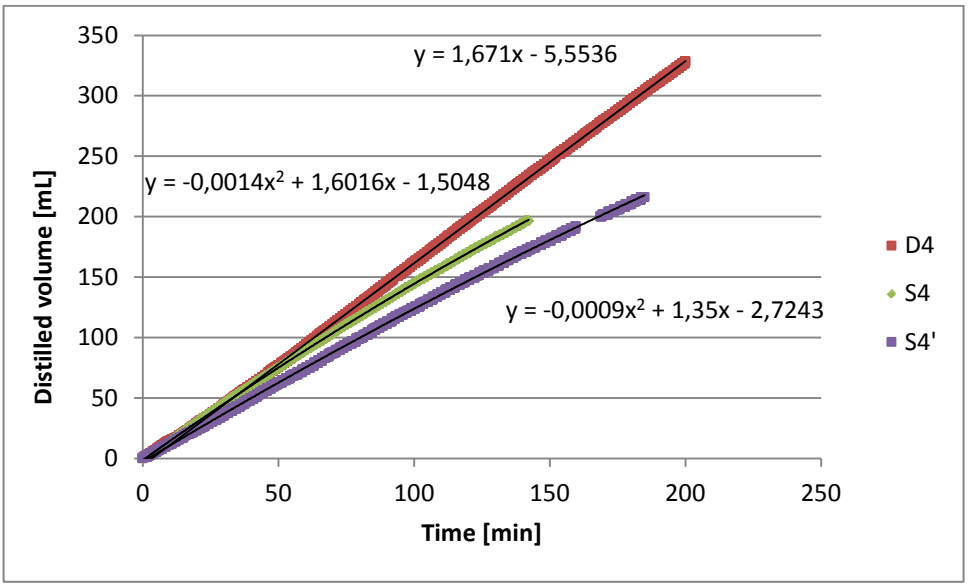

Figure 7-12 Distillate volume in D4, S4 and S4'

7.1.3. Concentration experiments with RO Brine (series A)

In these series, RO brine was used as feed solution, without any kind of pretreatment. The operating temperatures were kept the same and the flow rate and the use of spacers were the variables to study.

The composition of the RO brine from the DWTP of Sant Joan Despi can be seen in Table 5-1, as the brine is obtained in the desalination of a river water its salt content is not very high (TDS=6700 mg/L) but the presence of carbonate and calcium can result in the formation of scaling. The antiscaling agent, a polyphosphonate type (added in the water treatment plant) delays the precipitation, but any further concentration step will reach the supersaturation of carbonates (e.g. $CaCO_3$ and $MgCO_3$). Brines used in the experiments are over saturated in $CaCO_3$, however, due to the presence of antiscalant solutions they were stable and formation of $CaCO_3$ was not observed. This presence of anti-scaling agent is including a limitation on the theoretical prediction of the formation of mineral phases using the solubility constants of the expected mineral phases.

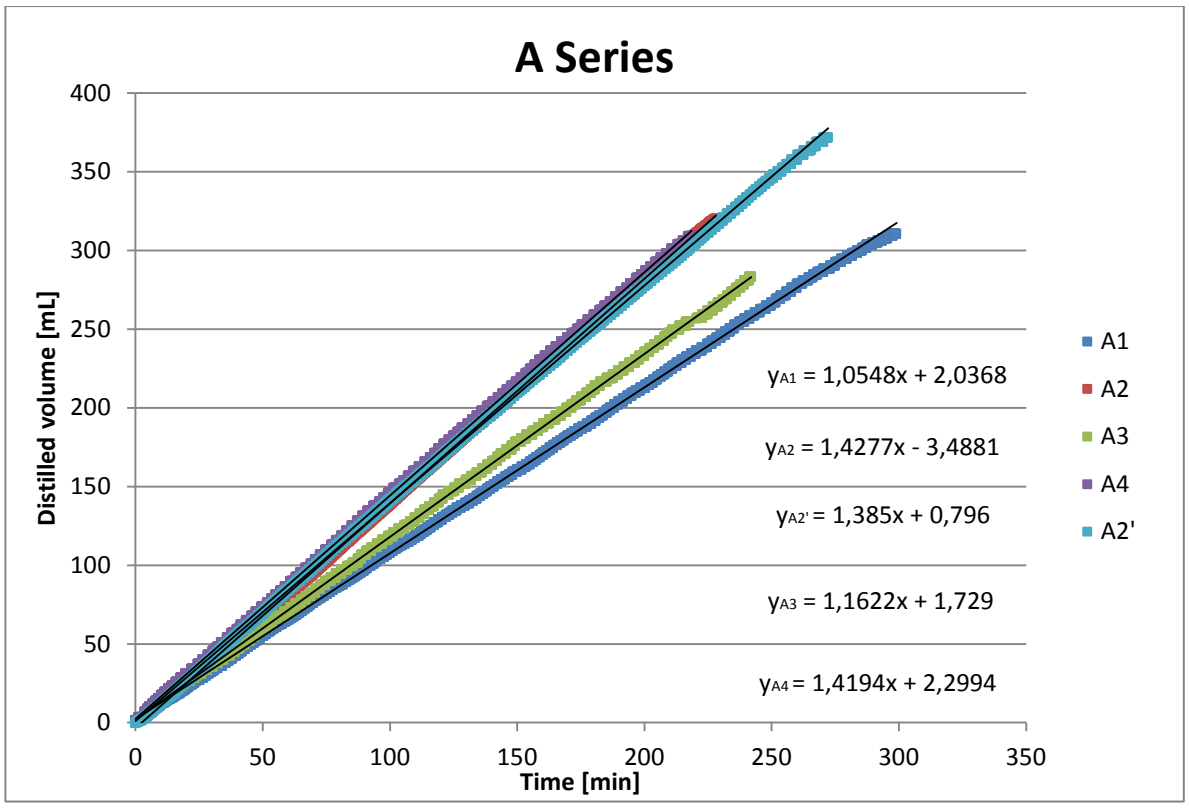

Figure 7-13 A Series results

The permeate fluxes follow the same order than in D Series and S Series, see Figure 7-13, but in these series there does not seem to be such a considerable gap between experiments 2 and 4, in fact the flow in A2' is higher than it A4. This is probably a consequence of variability, but for the next experimentation with treated brine conditions of experiment 2 will be used, as the presence of channel spacers has some technical difficulties attached with it, like more probabilities of having leaks in the module.

Scaling does not play a role as important as in S Series. In fact the distillation curve can be approximated as a straight line with satisfactory results (e.g. according to the regression coefficient R^2) as seen in Figure 7-13. At the end of the experiments, after 250 minutes, a slight deviation can be seen. Scaling at this point starts gaining importance by decreasing membrane's permeability. Concentration and polarization of the concentration also start being relevant at these concentration factors. If the experiments had been longer (e.g. up to hundreds of hours) then scaling would be much relevant, but with short-run experiments carried out in the scope of this project only with brines of higher concentrations it could be possible to observe flux decay.

If the case of maintaining the feed solution distilling or when a batch was distilled with the same membrane these three phenomena would suppose a higher reduction of the permeate flux and a reduction of the linear dependence of the distilled water volume with time.

	T_{fi} [°C]	T_{fo} [°C]	T_{bf} [°C]	T_{pi} [°C]	T_{po} [°C]	T_{bp} [°C]
A1	54	47	**50.5**	20	26	**23**
A2	52	49	**50.5**	21	25	**23**
A2'	52	49	**50.5**	20	24	**22**
A3	53	46	**49.5**	20	28	**24**
A4	51	47	**49**	20	24	**22**

Table 7-9 Operating temperatures of the A Series

If the temperatures of A Series in Table 7-9 are compared with the temperatures of D Series in Table 7-4, these are clearly of the same order and so it is possible to compare their permeate fluxes directly, see Figure 7-14.

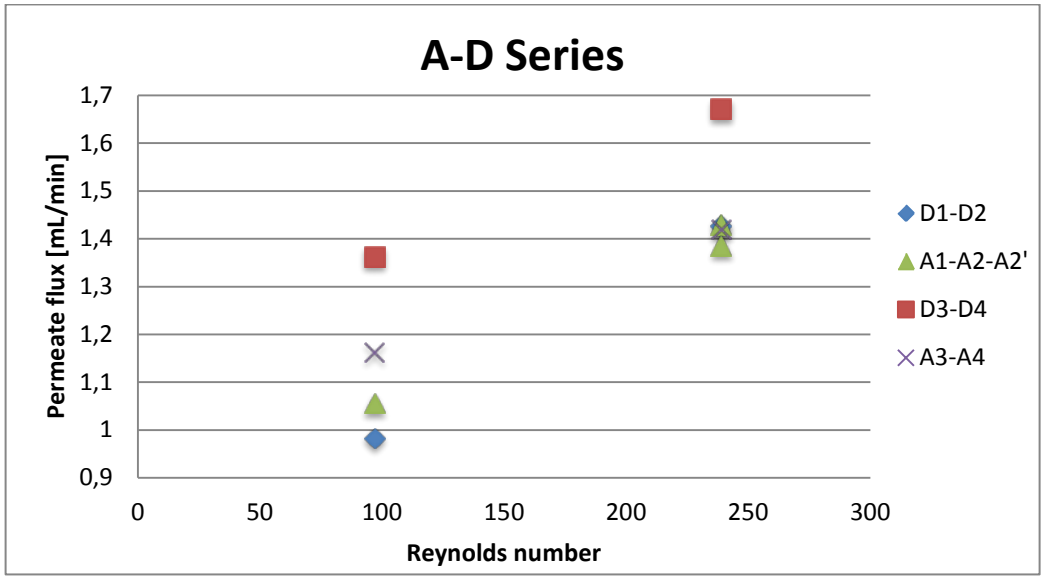

Figure 7-14 Comparison of the permeate flux for A and D Series

The Reynolds number in Figure 7-14 is real only when spacers were not used but as the flow rate is the same it is easier to attribute the same Reynolds number in order to compare results.

Overall, those experiments with distilled water have a higher permeate flux than those with brine. This is a consequence of the three phenomena already explained: membrane blocking, vapor pressure reduction due to the presence of salts and concentration polarization, which increases the later effect.

But in A1 the permeate flux is higher than D1. This could not be explained according to the defined basis, as in D1 and A1 the differences should be more accentuated due to the highly laminar flow. The explanation for this result should be associated to the observed variability between experiments. Even though, it should be mentioned that a continuous and highly accurate control of permeate mass was carried out, temperatures were recorded manually with an error of +/-1^{o}C. In addition, the flow rate was measured manually only once at the beginning of the experiment.

Once the operating variables were chosen A2 was repeated but this time samples were taken not only for analyzing the inorganic carbon but also to study the evolution of the brine composition using ion chromatography. The results of the initial and final concentrations can be seen in Table 7-10. With these concentration values the concentration factor for each species can be calculated in each moment, see Figure 7-15. The theoretical concentration factor is followed by most ions but not for the case of two: calcium and carbonate. This is clear evidence that between minute 0 and minute 60 precipitation of calcium carbonate begins. The other species do not precipitate, although small deviations from the expected concentration were measured. Differences encountered were associated to the dilution factors used in the chromatographic analysis. Then, an effort should be done in increasing the accuracy on the samples preparation by reducing the dilution factors to lower than 50.

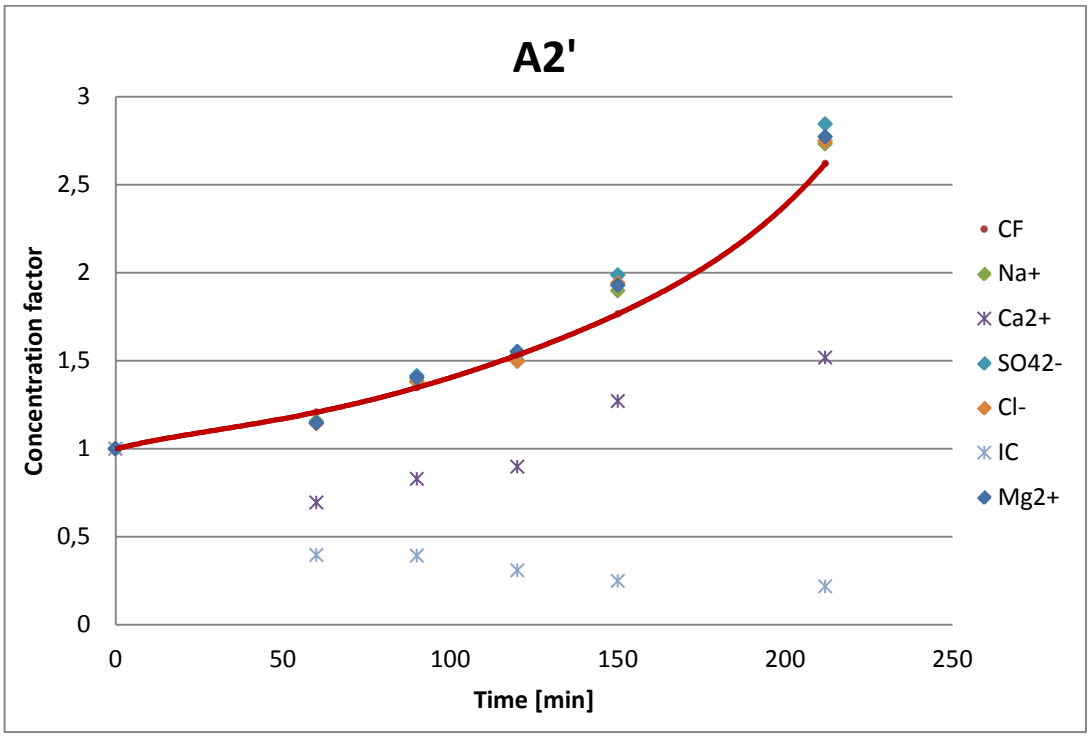

Figure 7-15 Concentration of each species along time

	Initial concentration [ppm]	Final concentration [ppm]
Na^+	985	2690
Ca^{2+}	574	871
Mg^{2+}	283	783
SO_4^{2-}	1664	4734
Cl^-	1536	4223
IC	392	85

Table 7-10 Initial and final concentrations of the main species of A2'

Inorganic carbon concentration decreases throughout all the distillation whereas calcium concentration decreases only in the first 60'. This is the result of two different phenomena:

- On one hand, dissolved CO_2 escapes the feed solution in the container when samples are taken and through the membrane pores. The CO_2 that leaves through the membrane pores is absorbed in the permeate solution, acidifying it. This explains why permeate had pH values as low as 6.13 that cannot be explained by contamination because the brine has alkaline pH values. Similar results have been reported in the literature by Warsinger (Warsinger et al., 2014). The conductivity of permeate was also higher due to the higher concentration of ions, an average of ten times higher than S Series (70 µS/cm versus 7µS/cm). Values measured however are explained to the increase of the CO_2 content, but not by the transport of brine neither through the pores nor through any membrane imperfection (e.g. holes).

- On the other hand, precipitation takes place, diminishing the amount of calcium and inorganic carbon in the feed solution. Precipitation occurs first at the point with lower temperature and higher concentration: the membrane surface.

These two phenomena combined have a result of a continuous decreasing concentration of inorganic carbon and continuous increasing of pH. But calcium does not always decrease, at some point it starts increasing its concentration. This recovery takes place because precipitation is dependent on both calcium and carbonate concentration, if carbonate concentration is very low calcium will be able to concentrate without precipitating.

7.2. Concentration experiments with pre-treated RO Brines (B, NN and MM series)

These series were carried out with brine pretreated with different combination of methods. B series were acidified and then distilled. NN were acidified and then bubbled in the aeration column. MM series include raw aeration and aeration followed by filtration and acidification.

Membrane Distillation was done with spacers and high flow rate, but the initial volume was not 500 mL like in previous series, it was 930 mL, the maximum volume of the container and the hot circuit. This was done in order to obtain higher concentration factors and promote precipitation, at the cost of making the experiments longer.

7.2.1. Concentration experiments with acidified RO Brines (B Series)

B series consist on two experiments: B1 and B2. Both without using spacers and with high flow rate, but the first with a total batch volume of 500 mL and the later with 930 mL. The feed solution consists in brine acidified down to a pH of 4±0.2. The pH was not easy to adjust because pH=4 is the point where the module of $\frac{d(pH)}{d(V_A)}$ (V_A stands for volume added of acid) has a higher value, and so just a drop of the HCl solution used could drastically change the pH (see Figure 7-16). The mean consume of HCl 37% was 4.3 mL per liter of brine.

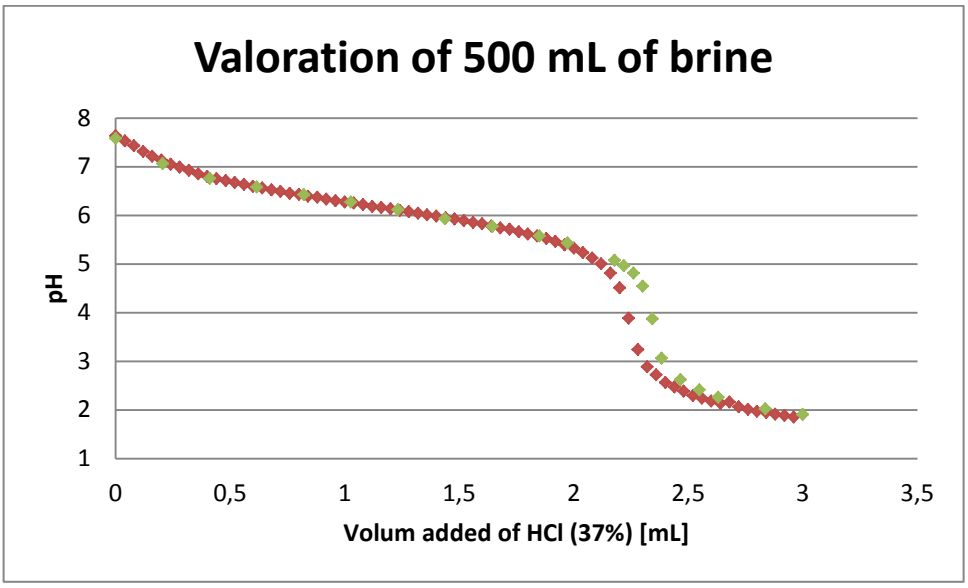

Figure 7-16 Results of two valorations of 500 mL of brine with 37%wt HCl

In Figure 7-17 the resulting distillation curves can be appreciated. At first sight, they seem to be the result of two different experiments with different conditions. As preliminar hypothesis this difference in slope is a consequence of the variability induced by the peristaltic pumps.

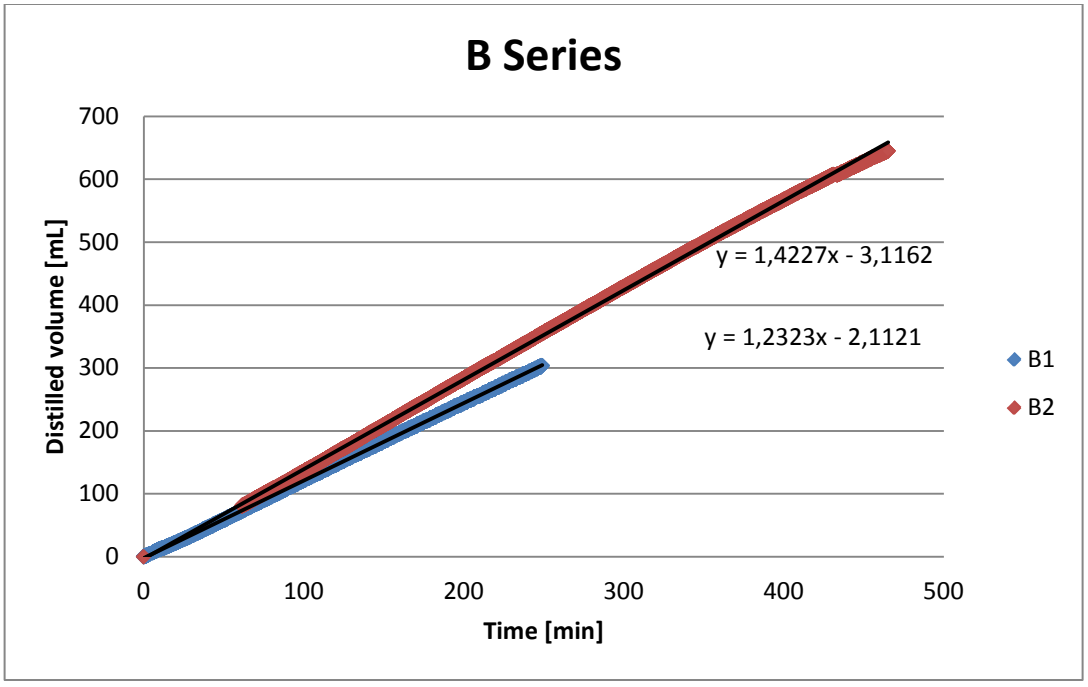

Figure 7-17 Distillation curves of B1 and B2

The average permeate flux was 1.33mL/min; whereas A2's average permeate flux was 1.41 mL/min. As expected, there is not a significant difference between them, as the operating temperatures are of the same order and the feed solution has a similar composition.

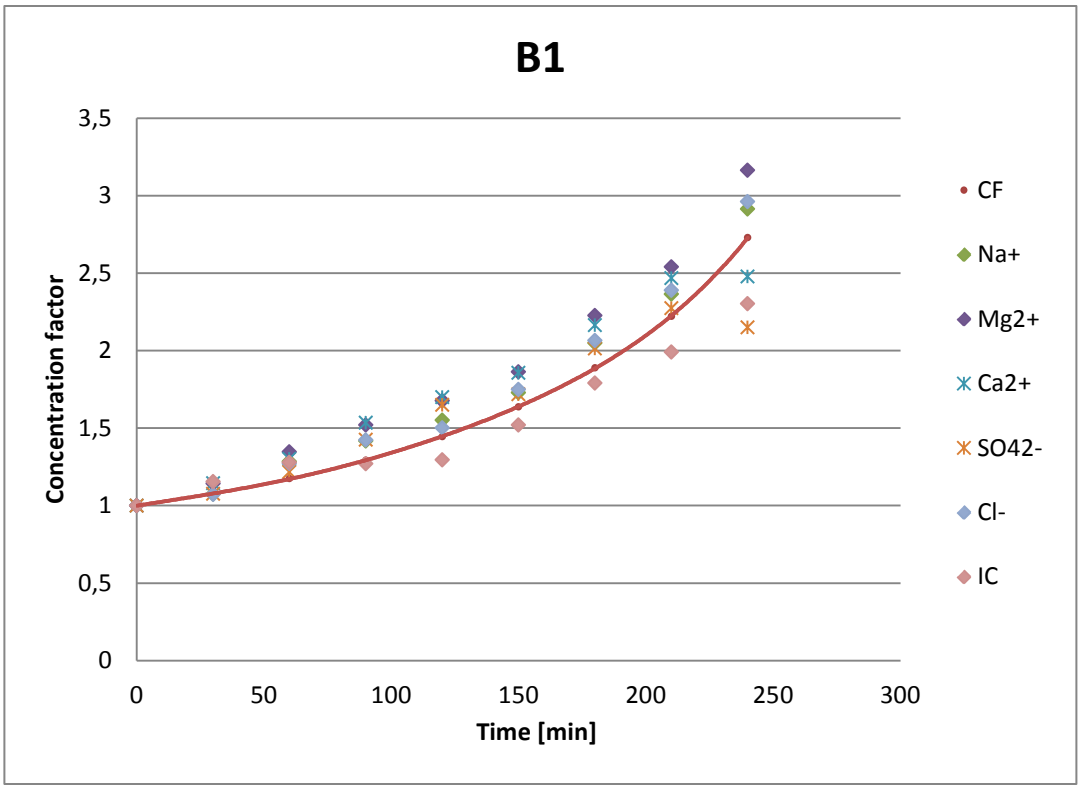

Figure 7-18 Concentration of each species through time for B1

In B1, the concentration factor of all species follows the theoretical concentration factor calculated with the amount of distilled volume, see Figure 7-18. However, in the last sample, the concentration factor of Ca^{2+} and SO_4^{2-} is minor than expected, this could be a hint that calcium sulfate precipitates, despite precipitate not being observed throughout the experiment. In Table 7-11 the initial and final concentrations can be seen, they resemble the concentrations from A2' except for Cl^-, Inorganic Carbon, SO_4^{2-} and Ca^{2+}. The initial concentration of Inorganic Carbon is only 16% of the A2's initial concentration. On the other hand, Cl^- has a higher initial concentration due to the addition of HCl. SO_4^{2-} lower final concentration is a consequence of the precipitation of $CaSO_4$, but the effect of this precipitation on the final concentration of Ca^{2+} is not as strong as the final concentration of Calcium is higher than in A2'.

	Initial concentration [ppm]	Final concentration [ppm]
Na^+	988	2880
Ca^{2+}	864	2142
Mg^{2+}	270	856

SO_4^{2-}	1596	3432
Cl^-	2515	7448
IC	64	147

Table 7-11 Initial and final concentrations for B1

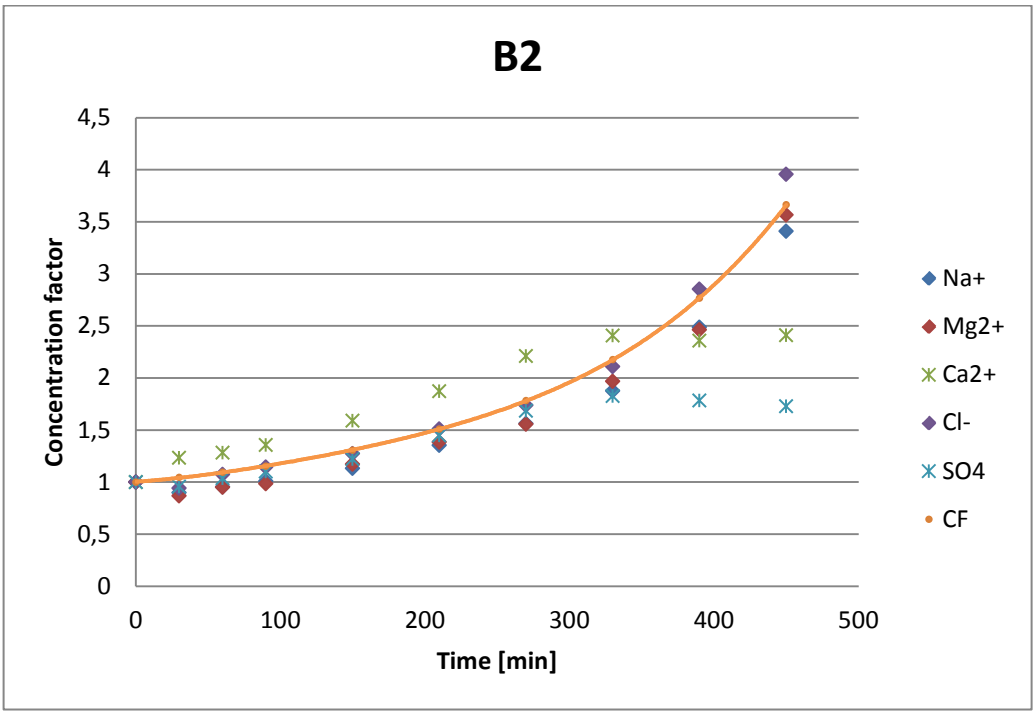

Figure 7-19 Concentration of each species through time for B2

Same applies for experiment B2, but in a much more clear way, as the concentration factors are higher because of the choice of distilling a higher volume of feed solution. Calcium and Sulfate concentration factors follow the theoretical concentration factor up to a certain point and then slightly decrease, see Figure 7-19. In Table 7-12 the initial and final concentrations for B2 can be seen, and they follow the same tendencies than in B1.

	Initial concentration [ppm]	Final concentration [ppm]
Na^+	868	2961
Ca^{2+}	522	1259
Mg^{2+}	212	755
SO_4^{2-}	1666	2877
Cl^-	2445	9672
IC	-	-

Table 7-12 Initial and final concentrations for B2

The maximum concentration factor without precipitation can be seen in Table 7-13. The two values for B1 and B2 resemble so much because they do not depend on the initial volume of feed solution.

	B1	B2	Mean
CF	2.18	2.22	2.20

Table 7-13 Concentration factors

7.2.2. Concentration experiments with acidified and aerated RO Brines (MM1, MM2 and NN Series)

These experiments consist in:

- MM1: Membrane Distillation of pretreated brine (930 mL), first aerated and then filtrated.
- MM2: Membrane Distillation of pretreated brine (930 mL), first aerated, and then filtrated and acidified to pH=4.
- NN: Membrane Distillation of pretreated brine (930 mL), first acidified and then aerated.

The three aeration processes were done in the same column with a steady flow of air of 2 Nm^3/h throughout 40 minutes. The filtration process was done with a pump, creating suction through a filter of 0.2 µm. Acidification was carried out with HCl 1 M, prepared with HCl 37%. See Table 7-14. The consumption of acid was 1.05 mL per liter of brine in MM2 and 1.89 mL per liter of brine in NN, lower than that of only acidification, with a consumption of 4.3 mL/L.

	MM1	MM2	NN
HCl 37% used [mL/L]	-	1.05	1.89
Aeration	40 min. at 2 Nm^3/h	40 min. at 2 Nm^3/h	40 min. at 2 Nm^3/h
Filtration	Yes	Yes	Not necessary

Table 7-14 Resources used

The resulting permeate fluxes are very similar between them and so are the distillation curves. They also resemble the curves of B Series, A2 and A2'. Pretreatment does not seem to affect the efficiency of the permeate flux. See Figure 7-20.

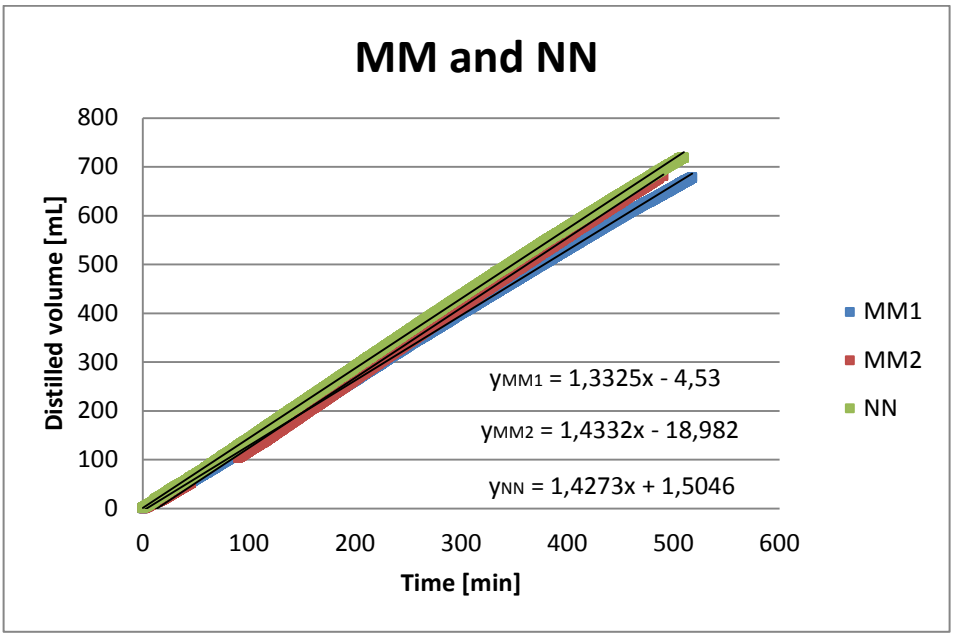

Figure 7-20 Distilling curves for each experiment

But pretreatments can affect strongly the concentrations of the species, delaying or accelerating precipitation. Precipitation may not be a problem when dealing with these low concentrated brines (e.g. in total inorganic carbon) and low volume batches, but for higher volumes of feed solution and longer runs it can be a crucial factor, this is why it has to be avoided or, at least, delayed.

In MM1 all species follow the theoretical concentration factor except for one: species with inorganic carbon (hydrogen carbonate, carbonate, carbonic acid and dissolved carbon dioxide). These species have a much more complicated system of equilibrium with the atmospheric carbon dioxide and cannot be expected to concentrate when distilled. At the end of the experiment calcium decreases its concentration factor, which means that has precipitated in form of $CaCO_3$. See Figure 7-21. This is confirmed with the SEM-XRI analysis, whose results can be seen in Table 7-15, in which the main components are C, O and Ca.

Spectrum	In stats.	C	O	Na	S	Cl	Ca	Total
Spectrum 1	Yes	27.95	45.47	0.46	3.55	0.64	21.93	100.00

Table 7-15 SEM-XRI qualitative analysis for MM1

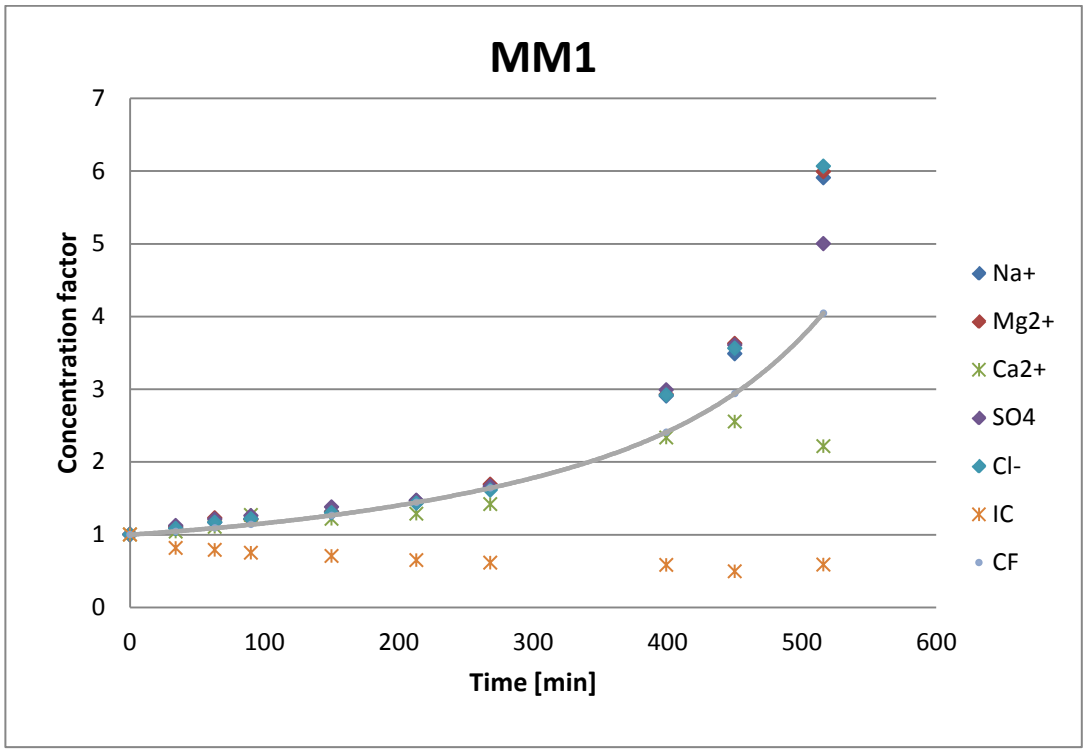

Figure 7-21 Concentration factors for MM1

The results are explained as preliminar hypothesis as calcium and carbonate are saturated at the end of aeration. Then this brine, with precipitated calcium carbonate, is filtrated. When the saturated brine is introduced in the container and heated, CO_2 leaves the feed solution (gases are less soluble with temperature) and the solubility of calcium carbonate is higher. The pKa's of the system also change. These effects combined explain why calcium carbonate does not precipitate immediately and calcium accepts a certain increase of concentration. This is known as thermal softening.

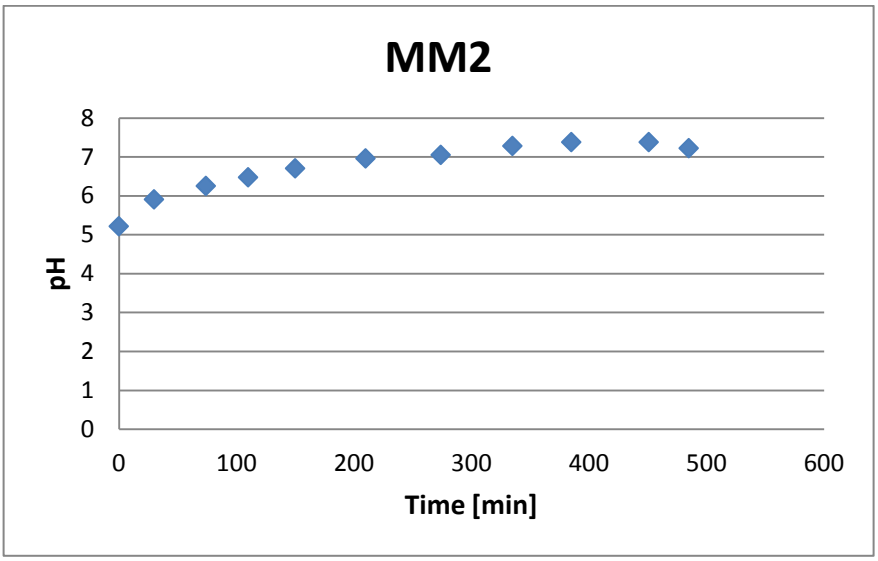

Figure 7-22 pH versus time in MM2

On the other hand, in MM2 inorganic carbon increases its concentration due to the acid pH, which increases over time, from pH=5.2 to pH=7.76, see Figure 7-22. This increase following the theoretical concentration factor of inorganic carbon is the consequence of carbonate being far away from the saturation point (the aerated and filtrated brine is acidified) and so it has a completely different equilibrium point, which changes over time when more and more volume of water is distilled.

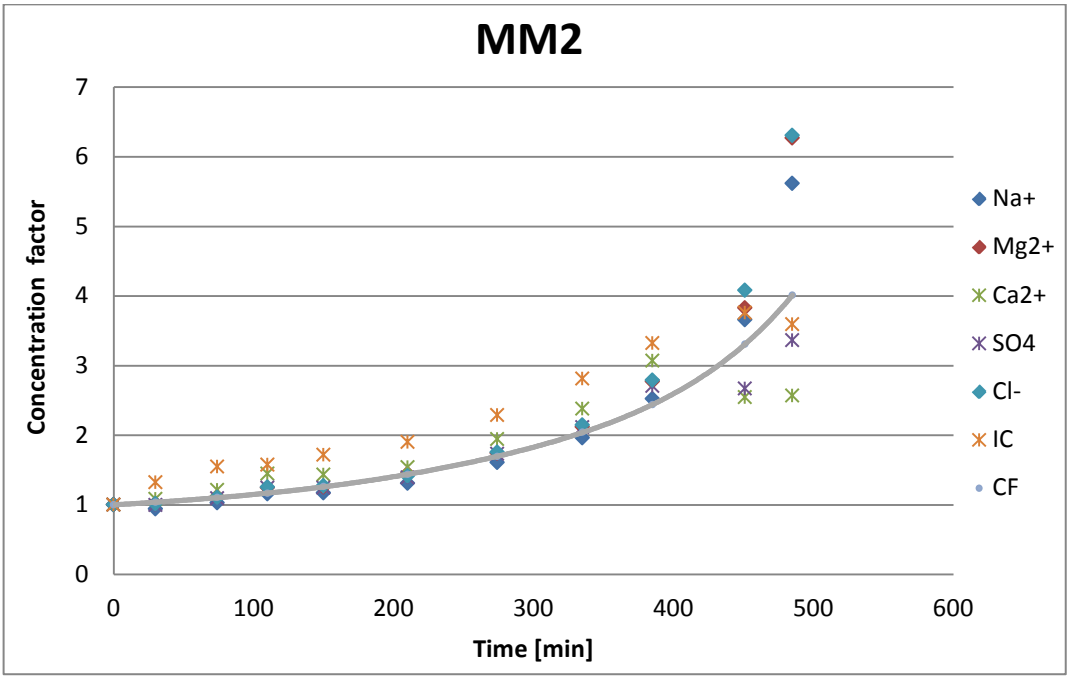

Figure 7-23 Concentration factors for MM2

The relevant conclusion is that both Calcium Carbonate and Calcium Sulfate precipitate, as there is a point in which all three inorganic carbon, calcium and sulfate change its tendency. See Figure 7-23.

In NN there is also clear precipitation, even not being observed on the membrane neither on the pipes, but it is not that clear of which component. What is clear is that Calcium is involved, and the concentration factor of chloride suffers a change too. As it is an acidified solution, the inorganic carbon also increases its concentration over time. See Figure 7-24. The SEM-XRI analysis (see Table 7-16) suggests that both Calcium Carbonate and Calcium Sulfate precipitate.

Spectrum	In stats.	C	O	Si	S	Ca	Total
Spectrum 1	Yes	12.65	56.81	0.22	13.91	16.41	100.00

Table 7-16 SEM-XRI qualitative analysis for NN

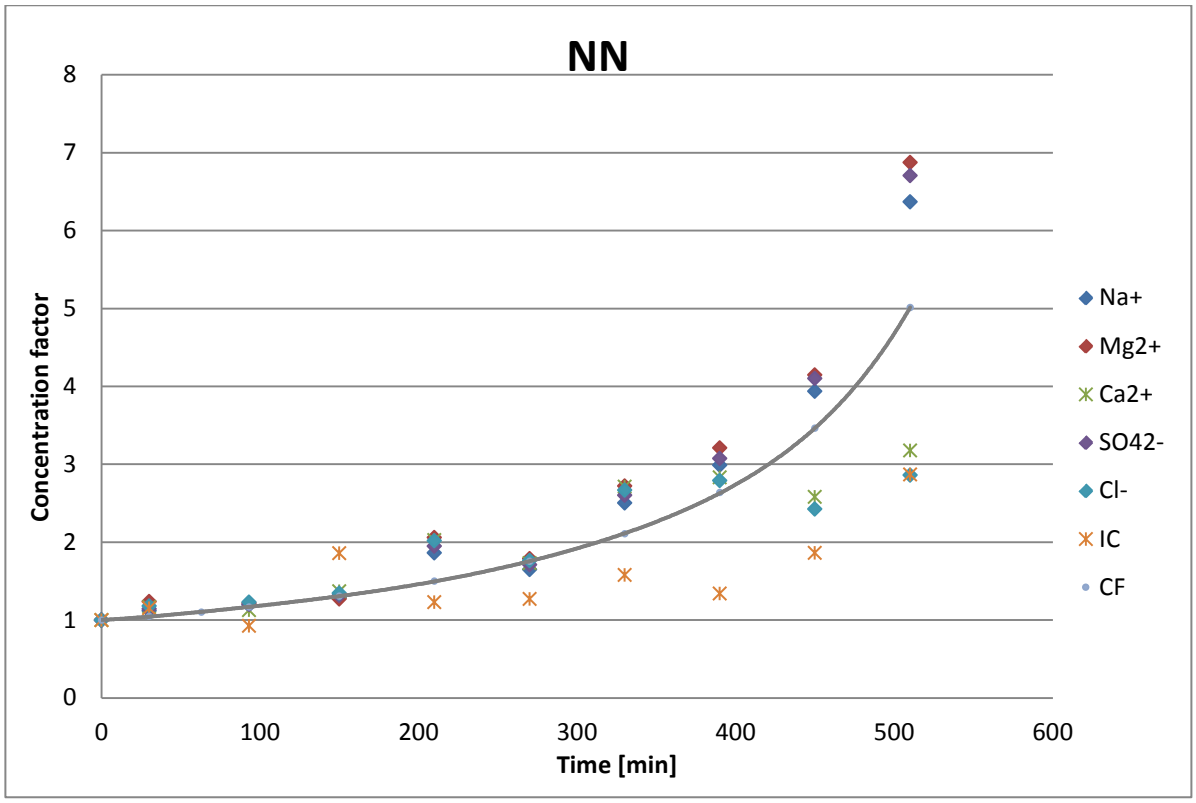

Figure 7-24 Concentration factors in NN

The maximum achievable concentration factor without precipitation has been calculated for the three pretreatments, see Table 7-17.

	MM1	MM2	NN
CF	2.94	2.44	2.63

Table 7-17 Maximum concentration factors

Comparing them with the concentration factors obtained with only acidification or with distilling raw brine, the three pretreatments can obtain a higher concentration without precipitation. Further study to identify the initiation of scaling formation should be done because the values in Table 7-17 can only give an approximated value of the concentration factor, the samples were taken every 60 minutes and the real point of precipitation cannot be found with these results.

If the initial concentration of Calcium was exactly the same in MM1 and in MM2 then it would be possible to assure that MM2 procedure can obtain a higher concentration factor than MM1 procedure. As it can avoid the precipitation of Calcium Carbonate and allows obtaining a higher concentration factor until Calcium Sulfate precipitates. But the concentration of Calcium is higher in MM2, and this might be the cause of the precipitation of Calcium Sulfate, see Table 7-18. To try to avoid these confusions, the pretreatments should have been applied to synthetic brines with known and equal concentrations, and then these solutions should have been distilled.

	MM1 I.C.	MM1 F.C.	MM2 I.C.	MM2 F.C.	NN I.C.	NN F.C.
Na^+	716	4232	904	5079	692	4406
Ca^{2+}	274	607	379	974	475	1508
Mg^{2+}	180	1078	211	1324	144	989
SO_4^{2-}	1527	7634	1683	5662	2081	13952
Cl^-	1398	8478	2063	13006	1399	4002
IC	154	91	26	94	4	12

Table 7-18 Initial and final concentrations of MM1, MM2 and NN series

7.3. Energetic efficiency

In this section the energetic efficiency of the module will be studied and then compared to other results from other DCMD modules and other MD configurations.

There are two major indicators of the energy efficiency of DCMD, one is the evaporation efficiency and the other one is the energy consumption per unit of volume of permeate.
It has to be stressed that these two indicators only consider the efficiency inside the module and do not take into account the efficiencies of the other equipment except for the pumps. The heat losses of the module are neither considered.

Series with NaCl feed solution have not been taken into account in this study as they have not been considered interesting and their calculus was way more complex and not constant through time. Series with distilled water as feed solution have neither been considered as this section is to compare desalination methods applied to brine.

The evaporation efficiencies for A-series can be seen in Table 7-19, as well as energy consumption per unit of volume of permeate. Even if it cannot be seen clearly with these experimental data, evaporation efficiency and energy consumption vary with the use of channel spacers, the regulation of feed solution and permeate flow rates and with the choice of temperatures of the inlets. In fact the results for A1 are clearly different to the others, being higher with a lower flow rate, just like found in the literature (Criscuoli et al., 2008).

So, the values obtained may be optimized with another choice of parameters. However, in the scope of this project, these values are only relevant to have a preliminar estimation of the efficiency and to be able to compare it to other desalination techniques; they are not aimed to study the dependency of efficiencies on other parameters.

	W_{pu} [W]	Flow rate [mL/ min]	Increase of temperature [^{o}C]	Energy transmitted to permeate [W]	Energy transmitted by condensation [W]	Energy consumption [kJ/Kg]	Evaporation efficiency [%]
A1	38	222	6	93	45	**2162**	**48**
A2	53	545	4	152	59	**2227**	**39**
A2’	53	545	4	152	58	**2296**	**38**
A3	38	222	8	124	48	**1962**	**39**
A4	53	545	4	152	59	**2240**	**39**
Mean	-	-	-	-	-	**2177**	**41**

Table 7-19 Efficiencies of A series

In order to calculate the efficiencies of Table 7-19, the increase of temperatures of the cold inlet and outlet were used instead of the decrease of the inlet and outlet of the hot side. This was done purposely to avoid counting heat losses to the environment as heat losses of conduction to the cold side.

(Bui et al., 2007) found E.E. in the range of 15% to 45% with lower operating temperatures and different types of hollow fiber modules, including modules working with PVDF membranes. (Criscuoli et al., 2008) found values of E.E. ranging from 20% to 39% for DCMD, being 39% the result of working with T_{mf}=59^{o}C and T_{mp}=14.3^{o}C in a counter-current flow flat sheet membrane module.

Comparing the mean value obtained of evaporation efficiency of 41% with the results from other publications dealing with DCMD it is possible to assure that they are very similar. However, if this same result is compared with the evaporation efficiency of VMD, the differences are not so small, VMD is reported to have evaporation efficiencies of up to 90% (Criscuoli et al., 2008).

The energy considered for the energy consumption calculus was only the necessary for the pumps to make the feed solution and permeate circulate in their respective circuits. The energy consumed by the pumps was estimated to be 53 W for the high flow rate and 38 W for the low flow rate. These values were estimated from the power of 70W of each pump and their respective controller's position. The energy necessary to heat and to cool the feed solution and permeate solution are not taken into account as they are considered to be obtained from residual waste sources with low operating temperatures.

Comparing the energy consumption is not easy as it depends a lot on which energies are considered. In other publications the energy consumptions are counted as the addition of the energy lost in the hot side of the module and the energy necessary to cool down the cold side of the module. (Criscuoli et al., 2008) used this criterion with results of 14400 kJ/Kg for DCMD, much higher than the 2177 kJ/Kg obtained with the module used in this work, in which only the energy spent on the pumps was considered. To be able to compare the results, the same criterion has been applied to A Series, see Table 7-20.

	A1	A2	A2'	A3	A4	Mean
Energy consumption [kJ/Kg]	**13539**	**13406**	**13820**	**13939**	**15091**	**13959**

Table 7-20 Energy consumption

This time it has been taken into account not only the energy necessary for the pumps but also energy to heat the feed from the temperature of the outlet to the temperature of the inlet and the energy to cool down the permeate from the temperature of the outlet to the temperature of the inlet. The mean value obtained is very similar to the one cited before from (Criscuoli et al., 2008). The pumping represents only a 16% of the energy.

One important consideration is the fact that it takes only 2594 kJ to heat and boil one kilogram of water at 20^{o}C at atmospheric pressure, whereas in MD it takes much more energy. The reason for that is the poor energetic efficiency of MD, in which more than half of the energy is lost in conduction heat and half of the energy actually spent in vaporization is spent on cooling the permeate. This is one of the main issues that for the last two decades different groups working in MD are trying to solve by designing more efficient modules.

If the value obtained of energy consumption is compared to the main implemented desalination techniques (see Table 7-21) it can be highlighted as incredibly higher than the other desalination techniques.

Reverse Osmosis	Mechanical Vapor Compression	Multi Stage Flash	Multi Effect Distillation	Membrane Distillation
4 kWh/m^3	**7 kWh/m^3**	**120 kWh/m^3**	**80 kWh/m^3**	**3890 kWh/m^3**

Table 7-21 Medium energy consumption values for different desalination techniques (Blank, Tusel, & Nisanc, 2007) (Reddy & Ghaffour, 2007) (Mabrouk, Nafey, & Fath, 2007)

Despite its incredibly high energy consume MD is still a promising desalination technique because of its low operating temperatures and pressures, which enable to obtain the energy from alternative energies or waste sources. For processes like RO or MED, there is not another way to obtain the high driving pressures or temperatures than the conventional. But MD could obtain its operating temperatures from solar collectors and the pumping could be generated by wind. This is the great advantage of MD, and not energetic efficiency, which is not relevant once the energy is provided by other means and there is efficient heat recovery (Susanto, 2011).

To make sure that the balance of heat is correct, two different values of conduction heat have been compared, as the conduction heat flow can be obtained in two different ways. The first is a theoretical estimation involving the thickness of the membrane, the membrane temperatures and the conductivity of the membrane, see Equation 4-8. The other is obtained subtracting the heat of vaporization from the total heat exchanged in the cold side, see Equation 4-6.

The results can be seen in Table 7-22. As exposed, the results have the same order and the same tendencies, but deviation is too high to be acceptable. These results show what has already been explained: the need of better flow rate control and measurement of temperatures in the inlets and outlets of the module. A better simulation should be done also, as the one made with the Matlab algorithm is using a simple approach, a finite element simulation would be much more suitable for the module.

	Theoretical conduction heat	Experimental conduction heat
A1	63 W	48 W
A2	71 W	93 W
A2’	76 W	94 W
A3	53 W	76 W
A4	70 W	93 W

Table 7-22 Results of conduction heat

8. Project planning and economic evaluation

8.1. Project cost: economic evaluation

Three different categories have been considered to have an estimation of the total cost of the project: Materials and Reagents, Energy consumption and Human resources.

Materials and Reagents used along the study are summarized in Table 8-1.

Material/Reagent	Amount	Unit cost	Total cost
Plastic stripes	1 bag	2 €	2 €
Plastic and silicone pipes	5 meters	3 €/m	15 €
PVDF membranes	25 units of 0.009 m^2	689 €/ m^2	155 €
Brine	100 L	0 €/L	0 €
Tap water	1 m^3	1.6 €/m^3	1.6 €
Distilled water	100 L	5 €/m^3	0.5 €
HCl 37%	200 mL	13.64 €/L	2.73 €
Household NaCl	0.7 Kg	0.25 €/Kg	0.175 €
Glass cell (broken)	1	8 €	8 €
Aeration column	1	80€	80 €
Base of PMMA	1	80 €	80 €
Air diffuser	1	5 €	5 €
Parafilm, nitril gloves…	x	x	5 €
Screws	x	x	15 €
Copper pipe	2m	4 €/m	8 €
Copper joint	10	1 €	10 €
			388 €

Table 8-1 Materials and reagents costs

In Energy Consumption all costs derived from the energy used by equipment are counted, see Table 8-2.

Equipment	Consumption	Unit cost	Total cost
Heated bath	140 kWh	0.15 €/kWh	21 €
Refrigerator	15.4 kWh		2.31 €
Agitator	9.8 kWh		1.47 €
Pumps	6.6 kWh		0.99 €
Compressor	4 kWh		0.60 €
			26 €

Table 8-2 Energy consumption costs

Human resources contain the salary of the two engineers working in this project, as well as their respective supervisors, see Table 8-3.

Position	Amount	Salary	Time	Total cost
Engineer	2	15 €/h	600 h	18000 €
Supervisors	3	40 €/h	40 h	4800 €
				22800 €

Table 8-3 Human resources costs

So the total cost associated of the project is 23210 €. This is just an estimation of the real cost of the project, as some of the individual contributions to the cost had to be estimated because there was not any record of the real cost. The real total cost of the project might be slightly higher or lower but of the same order.

8.2. Project planning

In Figure 8-1 there can be seen a Gantt diagram depicting the temporal planning of the project.

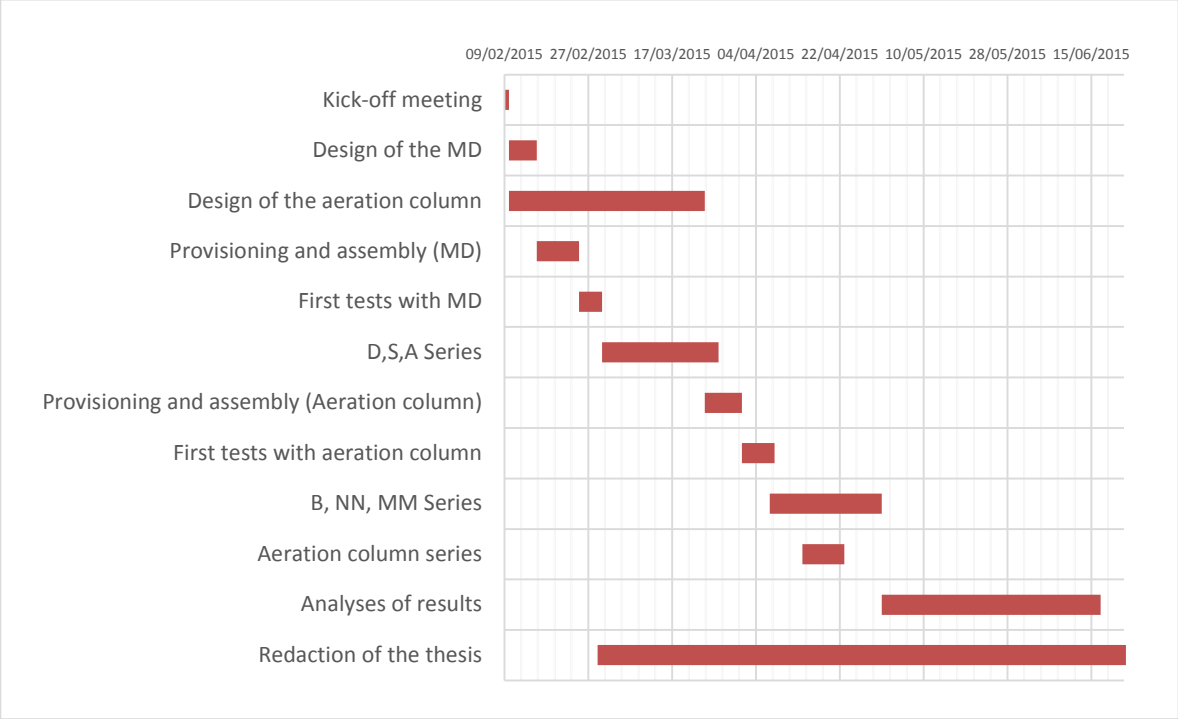

Figure 8-1 Gantt diagram of the temporal planning of the project

When planning the project, a solid order had to be followed; first all efforts had to be concentrated in designing and assembling the experimental set-up, and then it had to be tested. After, the

experimental phase could be started. The redaction of the thesis could start before having results by focusing on the literature search and the redaction of the state of the art.

9. Environmental impact; good laboratory practices

Throughout the realization of experimentation those solutions with an acid pH (lower than 4) were disposed in the container for residual pH solutions. The concentrated brines and feed solutions were disposed in the sink, as they do not suppose any contamination, and the volumes are minor than 200 mL. The solid residues like gloves, paper, the broken glass cell and the used membranes were disposed in the general waste.
As this project is purely experimental at laboratory scale no further study of environmental impact has been thought to be necessary.
If it was the case of an assembly at a higher scale, up to the point of pilot plant or bigger, the disposal of the brine should be studied if Zero Liquid Discharged was not achieved. These brines could potentially harm the environment.

But generally speaking, MD is a process from which a valuable product as pure water is obtained from a waste source of prime matter and a waste source of energy. So without any doubt it is possible to assert that the environmental impact would be reduced by its implementation.

10. Conclusions

Temperature and concentration polarization have been evaluated, temperature polarization has been found to be a crucial factor for the maximization of permeate flux, whereas concentration polarization is not relevant in terms of permeate flux but of promoting precipitation on the membrane.

The membrane transport parameters have been calculated from experimental data and compared to other works with very similar results.

The energy efficiency has been evaluated, and it has been found that MD is probably one of the less efficient desalination techniques if not the least. But this low energy efficiency might not be relevant if there is a good system of heat recovery and alternative or waste energy sources; in MD the implementation of these is easier than in other processes due to the low operating temperatures and pressures.

The DCMD can be applied to the brine coming from the RO desalination process treating surface river water at the Sant Joan Despí drinking water treatment plant, but even if there are pretreatments applied to it there will still appear scaling problems. Pretreatments can delay the precipitation of salts up to a certain point, and, eventually, the salt to precipitate can change between pretreatments. As concentration factor results were quite similar, there has not been a clear choice of the best pretreatment. In any case the three combinations seem promising having in mind its lower consumption of chemicals and better performance than plain acidification. The concentration factors for each pretreatment have been calculated and special efforts should be done in the improvement of the analytical procedures to analyze the concentrations of ions in such concentrated solutions.

Regarding the pretreatment experimentation, it is primordial to highlight that the results are dependent on the concentration and composition of the brine. So a RO concentrate coming from another plant or another type of brine may have different results and different maximum concentration factors.

11. Proposal of continuity and suggestions of improvement

11.1. Proposal of continuity

MD is still an emerging technology, and there is yet a lot to do, but many publications deal only with DCMD configuration and in the majority only the working parameters are studied. Membrane, channel spacers and module design have yet to be studied deeply. Many promising configurations like VMD are also being understudied due to their difficulty of setting them in a laboratory. Membrane Distillation Crystallization would also be interesting to study by adding a crystallizer.

But with DCMD there could still be studied the energetic efficiency dependence with operating temperatures and flow rates, as well as the use of channel spacers.

Making longer runs could be useful to study scaling on the membrane, and periodic cleaning would also be interesting, as well as using different types of membranes.

Another feasible idea would be to work with different types of brines, or to study more pretreatments or combination of pretreatments. Incorporating filtration seems to be effective, and thermal softening has also a big effect, only the temperature necessary to work with MD has already a softening and delaying effect in the case of saturated solutions as showed in this work.

11.2. Suggestions of improvement

Some problems arose throughout the project; here are some suggestions to solve them and to improve the quality of the work:

1. Work with a more accurate and complex finite elements simulator such as ANSYS or COMSOL.
2. Use temperature probes instead of thermometers to gain more accuracy of temperature monitoring.
3. Thermally isolate the pipes of the inlet and outlet of the module up to the temperature probes.
4. Incorporate a flow rate measurer in both feed solution and permeate circuit.
5. Improve the overflowing method to obtain a steady drop by drop flow.
6. Incorporate a continuous pH meter with a data logger inside the permeate container and inside the feed solution container.
7. Incorporate a conductivity meter with a data logger inside both the permeate container and the feed solution container.
8. Get a trustfully balance that will not shut down unexpectedly.
9. Use a bigger feed solution container. A bigger capacity means bigger potential concentration factors.

10. Use a heating bath with control of temperature inside the feed solution container and not inside the heating bath in order to reach the desired temperature
11. Incorporate stirring inside the feed solution container, this way if the flow rate is very low the precipitate will not accumulate in the bottom of the container.
12. Calibrate the TOC analyzer and make sure it is calibrated when using it.
13. Work with a smaller aeration column or obtain bigger volumes of brine.
14. Make sure that the compressor is going to work the full 45 minutes or make it work less time.
15. Think about an experimental procedure to obtain more values of concentration through time, if not continuous.
16. Work with a more concentrated solution than the brine but less than the NaCl solution to study deeper concentration polarization and flux decay.

12. Acknowledgements

First of all I want to thank the help and support that I have received throughout the project from my TFG director José Luis Cortina. I also want to thank my colleague Gerard Viader and the doctor Edxon Licón for all the moments shared together in the laboratory and the help and ideas that they have given me.

I wish to express my sincere thanks to the soon-to-be doctors Hermassi Mehrez and Mònica Reig for all their help to solve technical doubts. I am also grateful to the rest of laboratory colleagues for their support and company: Carlos, Neus, Sandra, Manuel, Genís, Adrià, Diana…

Finally, I. Lopez (Laboratory of Electronic Microscopy, Universitat Politècnica de Catalunya) for the FSEM analysis and to N. Moreno (IDAEA-CSIC) for XRD determinations.

I also want to express my gratitude to all the people that I have met over the years in the bachelor, without whom the degree would have been much heavier. I am also grateful to my family, who has kept encouraging me throughout all my life.

To everyone who, directly or indirectly, has helped me to be here now: my sincerely thanks.

Financial support for the project:

The experimental work has been carried out thanks to the funding provided by the Ministry of Science and Innovation through the ZERODISCHARGE project (CPQ2011-26799) and the Catalan government (project ref. 2009SGR905, 2014SGR050).
It is also acknowledge B. Lefevre and N. Arespaochaga from the Water Tecnology Center CETaqua and to J. Mesa from the Drinking Water treatment Plant of Sant Joan Despí for RO brines supply. The help of Benoit Lefevre on the design, integration and components supply of the MD set-ups is kindly recognized.

13. Bibliography

Ali, a., Macedonio, F., Drioli, E., Aljlil, S., & Alharbi, O. a. (2013). Experimental and theoretical evaluation of temperature polarization phenomenon in direct contact membrane distillation. *Chemical Engineering Research and Design*, *91*(10), 1966–1977.

Alkhudhiri, A., Darwish, N., & Hilal, N. (2012). Membrane distillation: A comprehensive review. *Desalination*, *287*, 2–18.

Andersson, S.-I., Kjellander, N., & Rodesjö, B. (1985). Design and field tests of a new membrane distillation desalination process. *Desalination*.

Blank, J. E., Tusel, G. F., & Nisanc, S. (2007). The real cost of desalted water and how to reduce it further. *Desalination*, *205*(1-3), 298–311.

Bui, V. A., Nguyen, M. H., & Muller, J. (2007). The energy challenge of direct contact membrane distillation in low temperature concentration. *Asia-Pacific Journal of Chemical Engineering*, *2*(5), 400–406.

Chan, M. T., Fane, A. G., Matheickal, J. T., & Sheikholeslami, R. (2005). Membrane distillation crystallization of concentrated salts - Flux and crystal formation. *Journal of Membrane Science*, *257*(1-2), 144–155.

Chiam, C.-K., & Sarbatly, R. (2013). Vacuum membrane distillation processes for aqueous solution treatment—A review. *Chemical Engineering and Processing: Process Intensification*, *74*, 27–54.

Cohen, Y., & Kirchmann, H. (2004). Increasing the pH of wastewater to high levels with different gases - CO2 stripping. *Water, Air, and Soil Pollution*, *159*(1), 265–275.

Criscuoli, A., Carnevale, M. C., & Drioli, E. (2008). Evaluation of energy requirements in membrane distillation. *Chemical Engineering and Processing: Process Intensification*, *47*(7), 1098–1105.

El-Bourawi, M. S., Ding, Z., Ma, R., & Khayet, M. (2006). A framework for better understanding membrane distillation separation process. *Journal of Membrane Science*, *285*(1-2), 4–29.

Elhajj, J., Al-Hindi, M., & Azizi, F. (2014). A Review of the Absorption and Desorption Processes of Carbon Dioxide in Water Systems. *Industrial & Engineering Chemistry Research*, *53*(1), 2–22.

Findley, M. E. (1967). Vaporization through Porous Membranes. *Industrial & Engineering Chemistry Process Design and Development*, *6*(2), 226–230.

Franken, a. C. M., Nolten, J. a. M., Mulder, M. H. V., Bargeman, D., & Smolders, C. a. (1987). Wetting criteria for the applicability of membrane distillation. *Journal of Membrane Science*, *33*(3), 315–328.

Greenlee, L. F., Lawler, D. F., Freeman, B. D., Marrot, B., & Moulin, P. (2009). Reverse osmosis desalination: Water sources, technology, and today's challenges. *Water Research*.

Gryta, M. (2008). Fouling in direct contact membrane distillation process. *Journal of Membrane Science*, *325*(1), 383–394.

Gryta, M. (2010). Desalination of thermally softened water by membrane distillation process. *Desalination*, *257*(1-3), 30–35.

Karakulski, K., & Gryta, M. (2005). Water demineralisation by NF/MD integrated processes. *Desalination*, *177*(1-3), 109–119.

Khayet, M. (2011). Membranes and theoretical modeling of membrane distillation: A review. *Advances in Colloid and Interface Science*, *164*(1-2), 56–88.

Lisitsin, D., Hasson, D., & Semiat, R. (2008). The potential of CO2 stripping for pretreating brackish and wastewater desalination feeds. *Desalination*, *222*(1-3), 50–58.

Mabrouk, A. A., Nafey, A. S., & Fath, H. E. S. (2007). Thermoeconomic analysis of some existing desalination processes. *Desalination*, *205*(1-3), 354–373.

Martinetti, C. R., Childress, A. E., & Cath, T. Y. (2009). High recovery of concentrated RO brines using forward osmosis and membrane distillation. *Journal of Membrane Science*, *331*(1-2), 31–39.

Martínez-Díez, L., & Vázquez-González, M. . (1999). Temperature and concentration polarization in membrane distillation of aqueous salt solutions. *Journal of Membrane Science*.

Pokrovsky, O. S. (1998). Precipitation of calcium and magnesium carbonates from homogeneous supersaturated solutions. *Journal of Crystal Growth*.

Qu, D., Wang, J., Fan, B., Luan, Z., & Hou, D. (2009). Study on concentrating primary reverse osmosis retentate by direct contact membrane distillation. *Desalination*, *247*(1-3), 540–550.

Reddy, K. V., & Ghaffour, N. (2007). Overview of the cost of desalinated water and costing methodologies. *Desalination*, *205*(1-3), 340–353.

Subramani, A., & Jacangelo, J. G. (2014). Treatment technologies for reverse osmosis concentrate volume minimization: A review. *Separation and Purification Technology*, *122*, 472–489.

Susanto, H. (2011). Towards practical implementations of membrane distillation. *Chemical Engineering and Processing: Process Intensification*, *50*(2), 139–150.

Warsinger, D. M., Swaminathan, J., Guillen-Burrieza, E., Arafat, H. a., & Lienhard V, J. H. (2014). Scaling and fouling in membrane distillation for desalination applications: A review. *Desalination*, *356*, 294–313.